Sexually dimorphic traits and male-specific differentiation are actively regulated by Doublesex during specific developmental windows in *Nasonia vitripennis*

Yidong Wang [a], Anna Rensink [b], Ute Fricke [a,*], Megan C. Riddle [c,$], Carol Trent [c], Louis van de Zande [b], Eveline C. Verhulst [a,d]

a. Wageningen University, Laboratory of Entomology, Wageningen, The Netherlands
b. Evolutionary Genetics, Development and Behaviour, Groningen Institute for Evolutionary Life Sciences, University of Groningen, Groningen, The Netherlands
c. Biology Department, Western Washington University, Washington, United States of America
d. Wageningen University, Laboratory of Genetics, Wageningen, The Netherlands

* Current address: Departement of Animal Ecology and Tropical Biology, Biocenter, University of Würzburg, Würzburg, Germany
$ Current addresses: Department of Psychiatry and Behavioral Sciences, University of Washington, Seattle, WA, United States of America; Eating Recovery Center
1231 116th Ave NE Suite 800, Bellevue, WA 98004

Corresponding author: eveline.verhulst@wur.nl

Keywords: *Nasonia,* Doublesex, sexually dimorphic traits, sexual differentiation, parasitoid wasps, sex determination

Abstract

Sexually dimorphic traits in insects are rapidly evolving due to sexual selection which can ultimately lead to speciation. However, our knowledge of the underlying sex-specific molecular mechanisms is still scarce. Here we show that the highly conserved gene, *Doublesex (Dsx),* regulates rapidly diverging sexually dimorphic traits in the model parasitoid wasp *Nasonia vitripennis* (Hymenoptera: Pteromalidae). We present here the revised full *Dsx* gene structure with an alternative first exon, and two additional male *NvDsx* isoforms, which gives important insights into the evolution of the sex-specific oligomerization domains and C-termini. We show the sex-specific *NvDsx* expression throughout development, and demonstrate that transient *NvDsx* silencing in different male developmental stages dramatically shifts the morphology of two sexually dimorphic traits from male to female, with the effect being dependent on the timing of silencing. In addition, transient silencing of *NvDsx* in early male larvae affects male genitalia tissue growth but not morphology. This indicates that male *NvDsx* is actively required to suppress female-specific traits and to promote male-specific traits during specific developmental windows. These results also strongly suggest that in *N. vitripennis* most sex-specific tissues fully differentiate in the embryonic stage and only need the input of *NvDsx* for growth afterwards. This provides a first insight into the regulatory activity of *Dsx* in the Hymenoptera and will help to better understand the evolutionary and molecular mechanisms involved in sex-specific development in this parasitoid wasp, which can eventually lead to the development of new synthetic genetics-based tools for biological pest control by parasitoid wasps.

Significance Statement

In insects, male and female differentiation is regulated by the highly conserved transcription factor Doublesex (Dsx). The role of Dsx in regulating rapidly evolving sexually dimorphic traits has received less attention, especially in wasps and bees. Here, we mainly focused on Dsx regulation of two sexually dimorphic traits and male genitalia morphology in the parasitoid wasp, *Nasonia vitripennis.* We demonstrate that *Dsx* actively regulates male-specific tissue growth and morphology during specific developmental windows. These findings will help to better understand the molecular mechanisms underlying the rapid evolution of sexual differentiation and sexually dimorphic traits in insects, but may also be the starting point for the development of new tools for biological control of pest insects by parasitoid wasps.

Introduction

Insects are well known for their distinct differences between male and female morphology.

The reproductive organs and sexually dimorphic traits such as wing shapes and colour patterns are one of the fastest evolving traits in insects. Therefore, they are often used to distinguish species, as these traits can differ dramatically between species. Development of these fast changing sexually dimorphic traits usually depends on specific genes that are expressed in a tissue and sex specific manner (1). Many of these genes are under control of the transcription factor, Doublesex (Dsx), that initiates sexual differentiation in insects (2–4). *Dsx* pre-mRNA is alternatively spliced to yield male-specific *Dsx* (*DsxM*) or female-specific *Dsx* (*DsxF*) transcripts, resulting in distinct sex-specific protein isoforms (5). Two functional domains are present in all insect Dsx homologs: 1) the DM domain which consists of a DNA binding domain (DBD) and an oligomerization domain (OD1) with a zinc module and binding sites to facilitate binding downstream targets, 2) a dimerization domain (OD2) with a common N-terminal part and a sex specific C-terminal part. These C-terminal sex-specific differences are assumed to be involved in the regulation of the development of sex-specific traits (6,7). For instance, in *Drosophila,* DsxM represses and DsxF activates the expression of *bric-à-brac (bab)* which results in male-specific abdominal pigmentation (8). A similar action of Dsx is observed in the formation of sex combs, an important feature for performing mating rituals in males of some *Drosophila* species (9). In *Bactrocera dorsalis, Dsx* knockdown in females triggers the interruption of yolk protein gene expression, leading to ovipositor deformation and a delay in ovary development (10). It confirms the essential role of DsxF to initiate and maintain female development in Diptera. In Lepidoptera (butterflies and moths) and Coleoptera (beetles), sex-specific *Dsx* expression in both sexes also affects many sex specific traits. For example, transient expression of *DsxM* in female *Bombyx mori* silkmoths distorts the development of female-specific genital organs by partially introducing male characters in female genitalia (11), whereas introducing mutations in the male-specific *Dsx* isoform of *B. mori* yields either malfunctioning males or intersexes (12). In *Papilio polytes* butterflies, differential expression of *Dsx* isoforms results in sex-specific wing patterns (13). *Dsx* also promotes the mandible growth in males but constrains it in females of *Cyclommatus metallifer* beetles (14). In *Trypoxylus dichotomus* beetles, the formation of head horns is antagonistically regulated by *DsxM* and *DsxF*, while the thoracic horn formation is *DsxM* independent (15,16). Noteworthy, all these experiments were conducted in a specific developmental stage and only few focused on sexually dimorphic traits. However, the expression of *Dsx* starts in early embryogenesis and continues through maturity which implies its ongoing action (10,17,18).

Thus far, the specific role of *Dsx* in regulating sexually dimorphic traits has not been studied in the Hymenoptera. *Dsx* sex-specific splice variants and expression differences have been

72 identified in honeybees, (*Apis mellifera*), bumble bees (*Bombus ignites),* Japanese ants
73 (*Vollenhovia emeryi*) and fire ants (*Solenopsis invicta*) (19–23), but the role of *Dsx* in
74 regulating reproductive organ development in males has only been shown in hymenopteran
75 sawflies, *Athalia rosae* (24). To understand the rapid evolution of sexual dimorphism in
76 insects and to compare the molecular mechanisms of *Dsx*-mediated regulation, it is
77 paramount to gain more knowledge on how *Dsx* directs sex-specific and sexually dimorphic
78 trait development in the Hymenoptera. Therefore, we set out to 1) identify the sex-specific
79 traits that are regulated by *Dsx* and 2) study the timing by which *Dsx* regulates these traits
80 during development in the parasitoid wasp *Nasonia vitripennis*.

81 *Nasonia vitripennis* belongs to the genus *Nasonia* (*Hymenoptera: Pteromalidae*), and has
82 become the model system for parasitoids as it is highly suitable for evolutionary and
83 developmental genetic studies. Multiple sexually dimorphic traits within the genus *Nasonia*
84 make it a perfect system to study sex differentiation (25,26). For instance, the femur of the
85 hind legs and the antennae of female *Nasonia* are pigmented with a dark-brown color,
86 whereas in males these are pale yellow (26). Only in *N. vitripennis,* males have dramatically
87 shorter forewings and are flightless (26), while the females can fly and have large forewings in
88 all species. Although *Dsx* has been identified in *N. vitripennis* (27), its role in regulating these
89 sexually dimorphic traits has not been shown before. Previous research identified one male
90 *Dsx* (*NvDsxM*) and one female *Dsx* (*NvDsxF*) splice variant (27) and showed that the
91 conserved splicing factor Transformer (Nvtra) is responsible for female-specific splicing of
92 *Dsx* transcripts, while in males the *Dsx* transcript is spliced by default into the male isoform
93 (28).

94 To assess the role of *Dsx* in regulating sexual dimorphism in *Nasonia,* we first revisited the
95 *NvDsx* genetic structure. We confirmed existing splice-variants and identified an alternative
96 starting exon and two additional male *NvDsx* splice-variants. We then used RNA interference
97 to temporally silence *Dsx* in different male developmental stages to study its function in
98 sexual differentiation and dimorphism. Ultimately, our results provide a great start to study the
99 molecular basis of sexual differentiation and rapidly evolving sexual dimorphism in insects in
100 general and particularly in the Hymenoptera.

101 **Results and discussion**

102 **Identification and characterization of two additional male-specific *Dsx* splice variants**

103 Previously, only one female (*NvDsxF*) and one male (*NvDsxM*) *Dsx* splice form were
104 identified in *N. vitripennis* (27). The *NvDsxF* splice variant shares the same first four exons

105 with the *NvDsxM* splice variant, but 108 bases are spliced out from exon 5 which leads to
106 female-specific exons 5F and 6F. In *NvDsxM,* exon 5M results from retaining this 108bp
107 intron, a form of alternative splicing which has not been observed for *Dsx* in other insects (27)
108 (Fig. 1, *NvDsxF* and *NvDsxM1*). This splice form translates into a Dsx protein with a very
109 short OD2 domain of only four amino acids (aa). The gene structure of this published *NvDsx*
110 does not resemble any other published *Dsx* structures. To investigate the possibility of
111 additional splice variants of *Dsx* pre-mRNA in *N. vitripennis,* we performed extensive 5' and 3'
112 RACEs. The results reveal a novel alternative starting exon that we designated exon 1' (Fig.
113 1). Note that the start codon of protein translation is in exon 2. Using RT-PCR to target exon 1'
114 to exon 5 we verified its presence in transcripts of both sexes but with a higher frequency in
115 female transcripts (Fig. S1). Alternative splicing at the 5' end has not been shown for *Dsx*
116 before. We assume that the alternative exon is used in all splice variants (Fig. 1), although
117 long-read RNA sequencing would be required to confirm this. From here on we refer to the
118 alternative variants collectively. The 3' RACEs identified two additional longer male splice
119 variants (Fig. 1). We designated the previously published male-specific variant *NvDsxM1* (M1:
120 NM_001162517; M1': MT043363); the newly found longer male splice forms were designated
121 *NvDsxM2* (M2: MT043359; M2': MT043360) and *NvDsxM3* ((M3: MT043361; M3':
122 MT043362). All male isoforms share the same exons 1 (or 1') to 5 with the female isoform
123 *NvDsxF* (F: NM_001162518; F': MT043364). The *NvDsxM2* open reading frame ends with a
124 stop codon in exon 8 and translates into a protein of 328 aa which is 105 aa longer than the
125 open reading frame of *NvDsxM1*. Compared to *NvDsxM2,* we find that exon 8 is spliced out in
126 *NvDsxM3* which puts the stop codon in exon 9 and yields a protein of 330 aa. These two
127 additional male specific splice variants skip the female-specific exon 6 completely which is a
128 shared feature of male splice forms in many insect species including fruit flies (*D.*
129 *melanogaster*) (29) (Fig. 1), wild silkmoths (*Antheraea assama*) (30), honeybees (*A. mellifera*)
130 (21) and fire ants (*S. invicta*) (20). We did not find any non-sex specific splice variants in *N.*
131 *vitripennis* as opposed to *A. mellifera* (Fig. 1) (21). NvDsxM2 and NvDsxM3 protein isoforms
132 are almost completely identical and only differ at the C-terminus after the male-specific OD2
133 domain (Fig. S6A).

134 ***NvDsxM2* and *NvDsxM3* are spliced by default**

135 To determine whether the additionally identified splice variants are exclusively expressed in
136 males, we first observed the overall expression of different *Nvdsx* splice forms in both males
137 and females. Across development, *NvDsxF* is only expressed in females while *NvDsxM1,*
138 *NvDsxM2* and *NvDsxM3* are highly expressed in males (Fig. S2), and expressed at a low

139 level in females. Only in males a slight increase of *NvDsxM1, -2 and -3* expression from 36h
140 toward the early pupal stage was observed. Afterwards, the expression remains relatively
141 constant until adult stage (Fig. S2). Overall, *NvDsxM2* is more abundant than *NvDsxM3* (Fig.
142 S2). Females express *NvDsxM1*, *NvDsxM2* and *NvDsxM3* at a low level probably due to
143 leaky default splicing of male-specific transcripts (Fig. 2B and Fig. S2).

144 We have shown previously that parental *Nvtra* RNA interference (RNAi) in the female pupal
145 stage leads to a shift in splicing from *NvtraF* to *NvtraM* (28). This subsequently induces a shift
146 from *NvDsxF* to *NvDsxM* (now *NvDsxM1*) splicing in both the treated adult females and the
147 offspring, without consequences for adult female fertility (28). The reduced levels of NvtraF
148 are no longer sufficient to regulate the splicing of all *Nvdsx* transcripts into the female-specific
149 form, leading to default expression of *NvDsxM1* splice variants. To verify the default and
150 NvTra independent splicing of *NvDsxM2* and *NvDsxM3*, we used *Nvtra* RNAi in the last larval
151 instar (4th instar) of females. RT-PCR was applied to amplify the different *NvDsx* and *Nvtra*
152 splice variants from 3 hours post injection (hpi) to 5 days post injection (dpi). After confirming
153 that *Nvtra* RNAi leads to *NvtraM* splicing in females (Fig. 2), we did not observe a clear
154 reduction of female *NvDsxF* expression, but a minor increase of *NvDsxM1* expression from
155 4dpi onwards was observed. *NvDsxM2* and *NvDsxM3* expression levels increase
156 substantially from 1dpi onward compared to *gfp* RNAi control (Fig. 2).

157 **NvDsxM represses female-specific pigmentation**

158 To assess the sex-specific function of Dsx, we studied the phenotypic effect of *NvDsx*
159 silencing at different developmental time points. We were unable to silence the male-specific
160 splice variants of *NvDsx* specifically (Fig. S3B), therefore we targeted the common region of
161 *NvDsx* (*NvDsxU*). We observed that the developmental stage at which *NvdsxU* dsRNA was
162 injected greatly influenced the expression levels of *NvDsx* measured using qRT-PCR. We
163 found no significant decrease of *NvDsx* expression in the 2nd instar *NvDsx* knockdown
164 (*NvDsxU*-i) male larvae in comparison to non-treated (NT) and *gfp* mock (*gfp*-i) when
165 sampling after the white pupal stage (Fig. S3*A*). The strong increase in *NvDsx* expression
166 from 4th instar male larvae onwards (Fig. S2) may be the main cause as the limited amount of
167 siRNA present in the 2nd larval instar is not capable of silencing the sudden increase of
168 transcript numbers in later developmental stages. However, this allows us to transiently
169 suppress *NvDsx* during different developmental time windows. Injecting *NvDsxU* dsRNA in 4th
170 instar male larvae led to a significant reduction of *NvDsx* in newly emerged adults when
171 compared with both NT (Tukey's HSD, P<.001) and *gfp*-i males (Tukey's HSD, P<.001) (Fig.
172 S3*B*). It confirmed a successful *NvDsx* knockdown starting in 4th instar male larvae with an

173 effect lasting into adulthood. The 4th instar *gfp*-i males also showed significant reduction of
174 *NvDsx* expression compared to NT (Tukey's HSD, P=0.021) suggesting that in the 4th instar
175 larvae there might be a non-target effect of *gfp* dsRNA as was shown before in the honey bee
176 (31) (Fig. S3*B*). Clear reduction was observed at the adult stage of pupal stage *NvDsxU*-i
177 males when compared to NT (Tukey's HSD, P=0.003) and pupal stage *gfp*-i males (Tukey's
178 HSD, P=0.002) (Fig. S3*C*) which indicates that we also obtained a highly significant
179 knockdown of *NvDsx* from the pupal stage onwards.

180 Non-treated and *gfp*-i males showed unpigmented antennae and legs (Fig. 3*A*, *B*, *C*),
181 whereas females have pigmented antennae and legs (Fig. 3*D*). *NvDsx* knockdown (*NvDsx*-i)
182 in 2nd instar male larvae increased the amount of pigmentation in the adults slightly (Fig. 3*F*),
183 but depleting *NvDsx* from 4th instar male larvae onwards increased pigmentation in their adult
184 stage to the point that it resembled female-like pigmentation (Fig. 3*E*). No pigmentation was
185 observed in adult males when *NvDsx* was depleted from the early white pupal stage onwards
186 (Fig. S4).

187 We did not find changes in pigmentation intensity by *NvDsx* RNAi experiments in 4th instar
188 female larvae (Fig. S5), and silencing *NvDsx* led to female-like pigmentation in males.
189 Therefore, we conclude that female pigmentation is the default developmental state, and in
190 males NvDsxM actively interferes with the melanin synthesis pathway. In *D. melanogaster,*
191 expression of sex-specific abdominal pigmentation is regulated by interaction of the HOX
192 protein Abdominal-B (Abd-B) and Dsx. Combined input of Abd-B and DsxF leads to the
193 expression of *bric-a-brac* (*bab*) which suppresses the pigmentation in the posterior abdomen
194 segments while DsxM represses *bab* to maintain the posterior abdomen pigmentation (8). As
195 we found no true intersex phenotype, we hypothesize that NvDsxF plays no role in enhancing
196 expression of the genes required for pigmentation in females. The slight reduction in antenna
197 pigmentation of 4th instar *NvDsx*-i males (Fig. 3E) is likely due to 1) a structural difference in
198 the antennae with males having less plate organs on the sub-segments than females causing
199 a different color reflection (32), and/or 2) incomplete knockdown of *NvDsx.* The deposition of
200 the pigments in the cuticle often starts from late pupal to early adult stages in *Drosophila* (33).
201 Therefore, initiating the RNAi response from 4th instar larva onwards creates enough time to
202 deplete *NvDsx* mRNA and NvDsx protein production to activate the expression of
203 pigmentation genes in *N. vitripennis* males.

204 ***NvDsx* silencing leads to increased forewing size of males**

205 The second sex-specific character that we assessed was forewing size and shape in

206 *N.vitripennis* adult males. Silencing *NvDsx* in both 2nd and 4th instar larvae resulted in
207 increased forewing length and width when compared to *gfp*-i (Tukey's HSD, P<0.001) and NT
208 males (Tukey's HSD, P<0.001) (Fig. 4*B* and *C*). Length/width (L/W) ratio of *NvDsx*-i
209 treatments also showed severe reduction compared to *gfp*-i (Tukey's HSD, P<0.001) and NT
210 males (Tukey's HSD, P<0.001) (Fig. 4*A*) indicating that the forewing became wider and more
211 female-like. However, the forewings of the *NvDsx*-i males were still smaller and narrower than
212 those of the NT females (Length: Tukey's HSD, P<0.001; Width: Tukey's HSD, P<0.001; L/W
213 ratio: Tukey's HSD, P<0.001) (Fig. 4*A*, *B* and *C*). Interestingly, here we found an effect of
214 timing as the forewing length and width increased significantly between 2nd and 4th instar
215 larvae *NvDsx*-i treatments in which earlier stage *NvDsx* knockdown led to more severe
216 changes (Tukey's HSD, P<0.001), steering the L/W ratio towards NT females dramatically
217 (Tukey's HSD, P<0.001). No significant differences were observed between 2nd and 4th instar
218 *gfp*-i males (Tukey's HSD, P=0.062), 2nd instar *gfp*-i and NT males (Tukey's HSD, P=0.070)
219 and 4th instar *gfp*-i and NT males (Tukey's HSD, P=0.999) (Fig. 4*A*, *B* and *C*). Depleting
220 *NvDsx* from the white pupal stage onwards had no effect on forewing size or shape in males
221 (Fig. S4).

222 Previous research showed that a non-coding region of *Dsx* in *N. giraulti*, termed wing-size1
223 locus (*ws1*), is correlated with the development of long wings in males, whereas the *ws1*
224 variant in *N. vitripennis* is correlated with the severely reduced forewing size in males (34).
225 Although higher *NvDsxM1* expression levels were detected in individuals with the *N.*
226 *vitripennis ws1* variant (34), the mechanism of *NvDsx* regulation is unclear and the *NvDsxM2*
227 and *-3* splice variants were unknown at the time. Our research confirmed that the regulation
228 of the male forewing size depends on high *NvDsxM* levels and illustrates the role of *NvDsxM*
229 in repressing wing growth. Changes in spatial and temporal expression of *unpaired-like* (*upd-*
230 *like*) has been shown to affect wing width in *Nasonia* males which is caused by multiple
231 regulatory changes (35). *NvDsxM* regulation is likely responsible for differentially expressed
232 *upd-like*. In contrast to the observed complete female-specific pigmentation after *NvDsxM*
233 depletion in 4th instar males, the depletion of *NvDsxM* from 2nd instar onwards is inadequate
234 to restore female forewing size. All these results suggest that forewing size and shape
235 development might already take place during embryonal development and our chosen time
236 window for RNAi is not early enough to induce a full switch. We cannot rule out antagonistic
237 effects of NvDsxM and NvDsxF on wing size development in *Nasonia*, since in females *Aedes*
238 *aegypti, Dsx* knockdown leads to smaller wing development (36). However, we observed no
239 wing size change after *NvDsx* knockdown in females (Fig. S5).

240 **Growth of male genitalia is controlled by *NvDsx***

241 Next, we assessed the role of *NvDsx* in male genitalia development and growth after
242 embryogenesis is completed by depleting *NvDsx* at either 2nd or 4th instar larval stage. This is
243 in contrast to many studies using genome editing in which *Dsx* is knocked out from early
244 embryogenesis onwards (10,12). *NvDsx*-i in both developmental stages reduced the
245 aedeagus length significantly when compared to *gfp*-i in both developmental stages and NT
246 males (Tukey's HSD, P<0.001) (Fig. 5A). *NvDsx*-i males from both developmental stages had
247 the same extent of aedeagus length reduction (Tukey's HSD, P=0.998). Aside from the
248 shortened aedeagus, the phallomere structure (genital phallic lobes) was also severely
249 reduced in size in both 2nd and 4th instar *NvDsx* depleted males (Fig. 5B-c and e) compared to
250 *gfp*-i and NT males (Fig. 5B-a, b and d), whereas the structure of the paramere including the
251 outer parameres, cuspis and digitus, was still intact (Fig. 5B). Compared to *gfp*-i males (Movie
252 S1), the severe length reduction of the aedeagus rendered *NvDsx*-i males unable to copulate
253 with females (Movie S2), showing that in this case size matters.

254 Dsx is shown to be involved in the differentiation of genitalia structures in male and female
255 insects in many cases by interactions with *HOX* genes during early embryogenesis (38).
256 However, whether *Dsx* is continuously required for genitalia development has not received
257 much attention. Previous studies using *Dsx* RNAi experiments in other species conducted at
258 late larval stages resulted in either deformed external genitalia or chimeras that contain the
259 structures of both sexes (24,39). Here, even though *NvDsx* RNAi was done at a distinctly
260 earlier stage (2nd larval instar) compared to other studied insect species, we did not observe
261 any abnormalities in genital organs other than size. This shows that contrary to other studied
262 insects, in *N. vitripennis* the differentiation of external genital organs is completed before the
263 2nd larval instar and only growth is required during later development. It also suggests that
264 besides the sex-specific tissue differentiation, *NvDsx* is required for the direct sex-specific trait
265 growth as it has been shown in stag beetles *Cyclommatus metallifer* where it was
266 demonstrated that *Dsx* can manipulate the sensitivity of JH in a sex-specific way to regulate
267 mandible growth in males and females (14).

268 **Evolution of Dsx sex-specific OD2 domains and C-termini**

269 Aligning the OD2 domains of NvDsxM1, NvDsxM2 and NvDsxM3 (Fig. S6A) or NvDsxF (Fig.
270 S6B) with other DsxM or DsxF OD2 domains, respectively, showed that across insect orders
271 the male-specific OD2 domain is far less conserved than the female-specific OD2 domain.
272 Within insect orders, also a strong reduction of the sequence identity in male-specific OD2
273 domain alignment was seen. This observed rapid evolution of male-specific *Dsx* regions is

supported by other research and is indicative of its fast evolution likely due to increased diversity of secondary sexual traits in male insects (40). In females, the sex-specific region of OD2 is relatively conserved across different insect orders. However, within the Hymenoptera, the female-specific OD2 domain showed a lower similarity. Only one out of eight conserved amino acids is being shared with all other tested species in the hymenopteran sequences, when compared to other insect orders that have half of the amino acids conserved (Fig. S6B). In *D. melanogaster* the C-terminus including the OD2 domain of DsxF binds the co-factor Intersex (41). The differences in female-specific OD2 amino acid composition in the Hymenoptera could indicate that either no co-factors or different co-factors play a role in regulating sexual development in this order compared to other insect orders. In addition, the female specific OD2 domain in the Hymenoptera was found to evolve much faster than the male-specific regions (40). This is contrary to Diptera, Lepidoptera and Coleoptera and has been suggested to correlate with the evolution of female-dominated eusociality and female-specific caste differentiation (40). However, *Nasonia* is solitary as are many other hymenopteran species. In the Hymenoptera, females arise from fertilized eggs while male development initiates by default from haploid, unfertilized eggs. We suggest that the rapid evolution of the female-specific OD2 domain in the Hymenoptera could be linked to this difference. All in all, the identification of the two additional male NvDsx isoforms opens the door to better comparative phylogenetic studies, and to better understand the evolution of *Dsx* in insects.

Outlook

In this research we identified two sexually dimorphic traits and one male-specific trait that are actively regulated during specific developmental windows by Dsx in *N. vitripennis.* Our results showed that male-specific lack of antennal and femur pigmentation is strictly regulated during pupal development as silencing *NvDsx* from the larval stage onwards resulted in build-up of pigmentation in the males, while silencing *NvDsx* from the pupal stage onwards did not have any effect. In addition, our results suggest that sex-specific wing size and shape is regulated by *NvDsx* during embryogenesis and early larval development. As silencing *NvDsx* from the 2nd larval instar onwards significantly increases wing size in males, while silencing from the pupa stage onwards does not change wing size and shape. However, *NvDsx* RNAi in the 2nd larval instar did not result in complete female-like wing size, indicating that the initial wing development occurs during embryogenesis and possibly the 1st larval instar. We additionally show that *NvDsx* regulates only male external reproductive organ growth and not morphology

308 from 2nd larval instar onwards, suggesting that the differentiation of external reproductive
309 organ tissue takes place before the 2nd instar which has not been reported before. Visualizing
310 *Dsx*-expressing cells in *D. melanogaster* has demonstrated that *Dsx* gene expression is under
311 elaborate temporal and spatial control to regulate tissue-specific sexual differentation (19).
312 Here, we expand this knowledge using a non-drosophilid species by showing that different
313 morphological characteristics require their own specific timing and action of Dsx protein and
314 we speculate that this timing and action is also species-specific. Our findings solidify the view
315 that in insects, sexual development is not only a set and forget mechanism that only operates
316 during embryogenesis, but one that requires continuous input from Dsx on a species-specific
317 basis.

318 **Material and methods:**

319 **Insects rearing**

320 The *Nasonia vitripennis* lab strain AsymCx was reared on *Calliphora sp.* hosts *at* 16h/8h
321 light/dark and 25℃. AsymCx strain is in the lab for over 10 years and cured from *Wolbachia*
322 infection.

323 **5' and 3' RACE-PCR to identify additional *NvDsx* splice variants**

324 For identification of the 3' ends of *NvDsx* mRNA*,* total RNA of 3 adult male- and female
325 AsymCx wasps were extracted individually using TriZol (Invitrogen, Carlsbad, CA, USA) and
326 cleared from genomic DNA by using the DNA-*free* DNA removal kit according to
327 manufacturer's instructions (Invitrogen, Carlsbad, CA, USA). Total RNA was annealed with
328 the 3' adapter from the FirstChoice RLM-RACE kit (Ambion, Austin, TX, USA) during the
329 reverse-transcription using RevertAidTM H Minus First Strand cDNA Synthesis Kit
330 (Fermentas, Hanover, MD, USA) and stored at -80°C. The cDNA was subjected to series of
331 (semi-) nested PCRs using primers complementary to the adapter and gene-specific primers
332 targeting NvDsxU, and NvDsx_X7, NvDsx_X8 and NvDsx_X9 at 94°C for 3 minutes, 35
333 cycles of 94°C for 30 seconds, 55-62°C for 30 seconds and 72°C for 2 minutes, with a final
334 extension of 10 minutes at 72°C. Primers were designed based on the initial *NvDsx* gene
335 structure (27) and sequences are listed in the Table S1.

336 For identification on the 5' end of *NvDsx*, total RNA of 3 female AsymCx wasps were
337 extracted using TriZol (Invitrogen, Carlsbad, CA, USA). After decapping, a 45-base RNA
338 adapter was ligated to the RNA population using the FirstChoice RLM-RACE kit (Ambion,
339 Austin, TX, USA) and reverse transcribed using the RevertAidTM H Minus First Strand cDNA
340 Synthesis Kit (Fermentas, Hanover, MD, USA). The cDNA was subjected to series of (semi-)

341 nested PCRs using primers complementary to the adapter and gene-specific primers
342 targeting *NvDsxU* at 94°C for 3 minutes, 35 cycles of 94°C for 30 seconds, 55-60°C for 30
343 seconds and 72°C for 2 minutes, with a final extension of 10 minutes at 72°C. Primers were
344 designed based on the initial *NvDsx* gene structure (27) and sequences are listed in the Table
345 S1.

346 5' and 3' RACE-PCR fragments were run and visualized on ethidium bromide-containing
347 1.5% agarose gel with 1×TAE buffer. All RACE-PCR products were purified using GeneJET
348 Gel Purification Kit (Fermentas, Hanover, MD, USA) and ligated into pGEM-T vector
349 (Promega, Madison, WI, USA) and transformed into competent JM-109 *Escherichia coli* cells
350 (Promega, Madison, WI, USA). Colony-PCRs were conducted by using primers
351 recommended by the kit at 94°C for 3 minutes, 40 cycles of 94°C for 30 seconds, 55°C for 30
352 seconds and 72°C for 2 minutes, with a final extension of 7 minutes at 72°C. All isoforms
353 were sequenced on an ABI 3730XL capillary sequencer (Applied Biosystems) and reads were
354 visualized and aligned in MEGA4 (42). Exon-intron structure of the genes was constructed by
355 aligning the mRNA sequences to *N. vitripennis* genome and visualizing in Geneious Prime
356 2019.1.3 and CLC Workbench 6.

357 **RT-PCR to confirm usage of alternative 1' exon**

358 Total RNA was extracted from four female samples and three male samples containing three
359 adults each using NucleoSpin XS (Brand) with final elution done in 15 µl nuclease-free water.
360 Eleven µl of eluted total RNA was converted to cDNA using RevertAidTM H Minus First
361 Strand cDNA Synthesis Kit (Fermentas, Hanover, MD, USA) with random hexamers
362 according to manufacturer's protocol and stored at -80°C. One female sample was not
363 converted to cDNA but used as gDNA contamination control in RT-PCR. The primer sets for
364 the RT-PCR reactions are: NvEF-1a and Nv_DsxU_F6 or Nv_DsxU_F7 with
365 Nv_Dsx_qPCR_R (Table S1). GoTaq® G2 Flexi DNA Polymerase (Promega) was used to
366 prepare the mastermix following manufacturer's instruction and amplified with a standard
367 PCR profile: 3 minutes at 95°C, 35 amplification cycles of 30 seconds at 95°C, 30 seconds at
368 55°C, 30 second at 72°C and a final extension of 7 minutes at 72 °C in a thermal cycler
369 (T100TM Thermal Cycler, Bio-Rad). Five µl of PCR product was visualized on a non-
370 denaturing 1% agarose gel with a 100bp ladder. PCR fragments were Sanger sequenced at
371 Eurofins Scientific to confirm the correct amplification.

372 **Alignment and phylogenetic analysis of Dsx OD2 domain across insect orders**

373 Dsx isoforms from 22 species across insect taxa were downloaded from NCBI protein
374 database with accession number attached in the end of each sequence name (Fig. S6A and
375 S6B). OD2 common domain and sex-specific region of OD2 domain selection is based on An
376 *et al*. 1996 (2). Both the male and female Dsx OD2 domain sequences were separately
377 aligned using Guidance2 Online Server with Guidance2 method, settings are MAFFT
378 algorithm, max iteration of 10, 100 alternative guide-trees. Geneious 2019.1 (created by
379 Biomatters. Available from https://www.geneious.com) was used to shade the amino acids
380 with Blosum62 score matrix applied to display the similarity between each sequence
381 (threshold at 3).

382 **RNAi of *NvTraF* and *NvDsx* gene**

383 For the *Nvtra* RNAi knockdowns, MEGAscript RNAi Kit (Thermo Fisher) was used to generate
384 dsRNA to target exon 5-8 of *Nvtra* mRNA in 4th larval instar females which resulted in a male
385 splice form of *NvDsx* as shown in Verhulst *et al.* (28). To conduct functional analysis of *NvDsx*,
386 same RNAi Kit was used to generate dsRNA based on either the common region of *NvDsx*
387 (exon 2-5) that presents in both male and female splice-variants or the specific region of
388 *NvDsx* (exon 7-9) that only presents in two longer male splice-variants. *Gfp* dsRNA was
389 generated from the vector pOPINEneo-3C-GFP which was a gift from Ray Owens (Addgene
390 plasmid # 53534; http://n2t.net/addgene: 53534; RRID: Addgene_53534). This *gfp* dsRNA
391 was used as control in all experiments as it has no target in *Nasonia*. Primers designed using
392 Geneious 10.0.9 to construct the dsRNA T7 template are listed in the Table S1. For male-
393 specific *NvDsx* RNAi, offspring of AsymCX strain was collected at 2nd and 4th larval instars
394 and white pupa stage which are described in Table S2. All dsRNAs were diluted with RNase-
395 free elution buffer (MEGAscript RNAi Kit (Thermo Fisher)) to 4000 ng/µl (NanoDrop™ 2000
396 Spectrophotometer, ThermoFisher) before proceeding to microinjection.

397 Microinjection of wasps was carried out with IM300 Microinjecctor (Narishige) and FemtoJet®
398 4i (eppendorf) and followed the protocols described by Werren *et al*. (43) and Lynch &
399 Desplan (44) with minor changes. Red colour food dye was pre-mixed with the dsRNAs in a
400 ratio of 1:9. Experiments were performed using AsymCx strain at different developmental
401 stages for different purposes (Table S3).

402 Second and 4th instar larvae were collected from parasitoid hosts and placed on a 1X PBS
403 agar plate before injection. Early pupal stage samples were fixed on the glass slides with
404 double-sided tape. After injection, 2nd instar larvae were transferred back to host (6-8 per host)
405 and sealed with the host shell. Afterward, sealed hosts were kept in 8 tube-PCR strips with

406 open lid. Subsequently, all injected samples either in 8 tube-PCR strip or on slides were
407 placed on 1X PBS plates to prevent dehydration and incubated at standard rearing conditions
408 until adult emergence.

409 ***NvDsx* splicing and expression throughout development**

410 Male and female wasps were separated at black pupal stage by the sex-specific traits such as
411 forewing size and presence/absence of the ovipositor. To generate female offspring, one
412 selected male and one selected female pupa were collected in a single glass vial clogged with
413 cotton plug until eclosion and kept for one more day to make sure they had mated. After
414 fertilization, two hosts per day for the first two days were provided to mated females to initiate
415 oviposition. Afterwards, one-hour host presentation was repeated twice in a row per day.
416 Since mated *N. vitripennis* tend to lay extremely female-biased eggs, offspring from mated
417 females was considered female (45). Male offspring was collected by using virgin females
418 with the same setup. To facilitate early stage (eggs) sample collection, egg-laying chambers
419 (1.5 ml Eppendorf tubes with cut-off tip presenting the head of host pupa plugged in 1000 µL
420 filter pipet tips) were made to allow the females only access to the head portion of the fly
421 hosts.

422 To confirm that male-specific splice variants are not under the regulation of NvTraF but splice
423 in default mode independently, female samples were collected from 3h, 1d, 2d, 3d, 4d, 5d and
424 6d after Nv*traF* knockdown. To study the expression pattern of *NvDsx* sex-specific splice
425 variants throughout whole developmental stages, samples were collected at specific time
426 points listed in Table S2. More than 50 embryo eggs were collected at 36h and five to 10
427 larvae, pupae or adults were collected at 2.5d and onwards. Collected samples were
428 subsequently frozen in liquid nitrogen and stored in -80°C. Sex-specific primers of *NvDsx*
429 were designed using Geneious 10.0.9. and are listed in the Table S1. Both *NvRP49* and
430 *NvEF-1a* were assessed for their expression stability in this semi-quantitative RT-PCR setup,
431 and *NvEF-1a* was finally chosen as the reference gene.

432 Frozen samples were homogenized by pestles which were designed for 1.5 ml
433 microcentrifuge tubes (Biosphere SafeSeal Tube 1.5ml). Total RNA was extracted using ZR
434 Tissue & Insect RNA MicroPrep™(Zymo) following manufacturer's instructions. On column
435 DNase treatment step was added to all samples. Subsequently, total RNA of each samples
436 was eluted in 16 µl of DNase/RNase free water. After verifying the purity and concentration by
437 NanoDrop™ 2000 Spectrophotometer (ThermoFisher), one µg of each template was
438 synthesized into cDNA with a standard reaction mix (SensiFAST™ cDNA Synthesis Kit,

439 Bioline) in a thermal cycler (Bio-Rad T100TM Thermal Cycler, Bio-Rad) with 5 minutes
440 priming at 25°C, 30 minutes reverse transcription at 46°C and 5 minutes reverse transcriptase
441 inactivation at 85°C.

442 For all RT-PCR reactions, GoTaq® G2 Flexi DNA Polymerase (Promega) was used to
443 prepare the mastermix following manufacture's instruction and amplified with a standard PCR
444 profile: 3 minutes at 95°C, 34 (male-specific splicing verification) / 29 (expression pattern of
445 *NvDsx*) amplification cycles of 30 seconds at 95°C, 30 seconds at 55°C, 50 seconds at 72°C
446 and a final extension of 5 minutes at 72 °C in a thermal cycler (T100TM Thermal Cycler, Bio-
447 Rad). In order to standardize the expression pattern of *NvDsx*, the number of PCR cycles
448 needed was determined by comparison of the brightness of the bands in gels from different
449 PCR reactions with cycles ranging from 25 to 34 to achieve non-oversaturated brightness. In
450 the end 29 cycles were used for both reference genes and target genes.

451 **Silencing efficiency of *NvDsx***

452 qPCR was conducted to verify the silencing efficiency of *Dsx* knockdown. After *dsRNA*
453 injection, samples were collected at either adult stages (injected at the 4th larval instar and the
454 white pupa stage) or the white pupa stage (injected at the 2nd larval instar). Four to five pupae
455 or adults were pooled to produce one biological replicate and six biological replicates per
456 treatment were prepared. All testing samples were used in qPCR according to SensiFAST^{TM}
457 SYBR® No-ROX Kit manual (Bioline). *NvDsx* qPCR primers were designed on the common
458 region (exon 2-5) of male and female splice variants (Table S1). *NvEF-1a* was used as
459 reference genes. qPCR was carried out using the CFX96TM Real-Time System (Bio-Rad)
460 with Bio-Rad CFX Manager 3.1 Software (Bio-Rad). The standard qPCR profile consists of
461 95°C for 3 minutes, 45 amplification cycles of 15 seconds at 95,15 seconds of 55°C, 30
462 seconds of 72°C and a final standard dissociation curve step to check for non-specific
463 amplification.

464 **Measurements of male forewing size, external reproduction organs**

465 Forewing size was measured by wing length and width based on the standard methods
466 described by Loehlin *et al.* (46). Tibia length of the hind leg was used to standardize the body
467 size differences among individuals (47). Forewings and external reproduction organ of adult
468 males were dissected on clean slides with a drop of 1 X PBS buffer using dissection tweezers
469 and subsequently mounted in a drop of ethanol on slides which was allowed to evaporate.
470 External reproduction apparatuses were identified based on the description in Liu *et al*. (48)
471 and E. Snodgrass (37). Photos were taken by Dino-Lite Edge 5MP digital microscope and

472 measured by using DinoCapture 2.0 software.

473 **Data analysis**

474 qPCR data was first imported to LinRegPCR software (LinRegPCR, 2017.1.0.0, HFRC,
475 Amsterdam, The Netherlands) (49). After baseline correction, the initial number of templates
476 (N0) were calculated based on the average PCR efficiency of each amplicon. Relative
477 expression levels of *NvDsx* in each sample was obtained by dividing the N0 value of *NvDsx*
478 by N0 value of *NvEF-1a*. Statistical analysis of qPCR and measurement data was performed
479 in R using One-way ANOVA and Tukey's Honest Significant Difference (HSD) for post hoc
480 test.

481 **Acknowledgment**

482 We thank Hans Smid for assisting with phenotype recording; Rutger Diepeveen for his
483 contribution to the *NvDsx* RNAi work; Joan Diaz Calafat, Age Muller, Simon Pleiter and Romy
484 Gielings for their contribution to the *NvtraF* RNAi work; Min Xu for supporting the sample
485 preparation, collection and measuring; and Weizhao Sun for recording the mating behavior of
486 RNAi treated males. We additionally thank all the tested *N. vitripennis* for their great sacrifice
487 to science. This work is part of the Dutch Research Council (NWO) research programme
488 Innovational Research Incentives Scheme Veni with project number 863.13.014 granted to
489 ECV.

490

491 **Reference**

492 1. O. Barmina and A. Kopp, Sex-specific expression of a *HOX* gene associated with rapid
493 morphological evolution. *Dev. Biol.* **311**, 277–286 (2007).

494 2. W. An, S. Cho, H. Ishii and P. C. Wensink, Sex-specific and non-sex-specific
495 oligomerization domains in both of the *doublesex* transcription factors from *Drosophila*
496 *melanogaster*. *Mol. Cell. Biol.* **16**, 3106–11 (1996).

497 3. J. N. Shukla and S. R. Palli, Doublesex target genes in the red flour beetle, *Tribolium*
498 *castaneum*. *Sci. Rep.* **2**, 948 (2012).

499 4. F. Ohbayashi *et al*., A homologue of the *Drosophila doublesex* gene is transcribed into sex-
500 specific mRNA isoforms in the silkworm, *Bombyx mori*, *Comp. Biochem. Physiol. - B Biochem.*
501 *Mol. Biol.* **128**, 145-158 (2001).

502 5. K. C. Burtis and B. S. Baker, *Drosophila doublesex* gene controls somatic sexual
503 differentiation by producing alternatively spliced mRNAs encoding related sex-specific
504 polypeptides. *Cell.* **56**, 997–1010 (1989).

505 6. D. C. Price, A. Egizi and D. M. Fonseca, The ubiquity and ancestry of insect *doublesex*. *Sci.*
506 *Rep.* **5**, 13068 (2015).

507 7. E. C. Verhulst and L. van de Zande, Double nexus-Doublesex is the connecting element in
508 sex determination. *Brief. Funct. Genomics* **14**, 396–406 (2015).

509 8. T. M. Williams *et al*., The regulation and evolution of a genetic switch controlling sexually
510 dimorphic traits in *Drosophila*. *Cell* **134**, 610–623 (2008).

511 9. A. Kopp, *Drosophila* sex combs as a model of evolutionary innovations. *Evol. Dev.* **13**,
512 504–22 (2011).

513 10. X. Chen *et al*., Disruption of sex-specific *doublesex* exons results in male- and female-
514 specific defects in the black cutworm, *Agrotis ipsilon*. *Pest Manag. Sci.* **75**, 1697-1706 (2019).

515 11. M. G. Suzuki *et al*., Role of the male BmDSX protein in the sexual differentiation of
516 *Bombyx mori*. *Evol. Dev.* **7**, 58–68 (2005).

517 12. J. Xu *et al*., Sexually dimorphic traits in the silkworm, *Bombyx mori*, are regulated by
518 *doublesex*. *Insect Biochem. Mol. Biol.* **80**, 42–51 (2017).

519 13. K. Kunte *et al*., *doublesex* is a mimicry supergene. *Nature* **507**, 229–232 (2014).

520 14. H. Gotoh *et al*., Developmental link between sex and nutrition; *doublesex* regulates sex-
521 specific mandible growth via juvenile hormone signalling in stag beetles. *PLoS Genet.* **10**,
522 e1004098 (2014).

523 15. Y. Ito *et al*., The role of *doublesex* in the evolution of exaggerated horns in the Japanese
524 rhinoceros beetle. *EMBO Rep.* **14**, 561–567 (2013).

525 16. C. C. Ledón-Rettig, E. E. Zattara and A. P. Moczek, Asymmetric interactions between
526 *doublesex* and tissue- and sex-specific target genes mediate sexual dimorphism in beetles.
527 *Nat. Commun.* **8**, 14593 (2017).

528 17. C. C. Robinett, A. G. Vaughan, J.-M. Knapp and B. S. Baker, Sex and the single cell. II.
529 There is a time and place for sex. *PLoS Biol.* **8**, e1000365 (2010).

530 18. J. L. Morrow, M. Riegler, M. Frommer and D. C. A. Shearman, Expression patterns of
531 sex-determination genes in single male and female embryos of two *Bactrocera* fruit fly
532 species during early development. *Insect Mol. Biol.* **23**, 754–767 (2014).

533 19. A. Klein *et al*., Evolution of social insect polyphenism facilitated by the sex differentiation
534 cascade, *PLOS Genet.* **12**, e1005952 (2016).

535 20. M. Nipitwattanaphon *et al*., Effects of ploidy and sex-locus genotype on gene expression
536 patterns in the fire ant *Solenopsis invicta*. *Proc. R. Soc. B Biol. Sci.* **281**, 20141776–20141776
537 (2014).

538 21. S. Cho, Z. Y. Huang and J. Zhang, Sex-specific splicing of the honeybee *doublesex* gene
539 reveals 300 million years of evolution at the bottom of the insect sex-determination pathway.
540 *Genetics* **177**, 1733–41 (2007).

541 22. A. Ugajin *et al*., Expression profile of the sex determination gene *doublesex* in a
542 gynandromorph of bumblebee, *Bombus ignites*. *Sci. Nat.* **103**, 17 (2016).

543 23. M. O. Miyakawa, K. Tsuchida and H. Miyakawa, The *doublesex* gene integrates multi-
544 locus complementary sex determination signals in the Japanese ant, *Vollenhovia emeryi*.
545 *Insect Biochem. Mol. Biol.* **94**, 42–49 (2018).

546 24. S. Mine *et al*., Identification and functional characterization of the sex-determining gene
547 *doublesex* in the sawfly, *Athalia rosae* (Hymenoptera: Tenthredinidae). *Appl. Entomol. Zool.*
548 **52**, 497–509 (2017).

549 25. R. Raychoudhury *et al*., Behavioral and genetic characteristics of a new species of
550 *Nasonia*, *Heredity.* **104**, 278–288 (2010).

551 26. D. C. Darling and J. H. Werren, Biosystematics of *Nasonia* (Hymenoptera: Pteromalidae):
552 Two new species reared from birds' nests in north America. *Ann. Entomol. Soc. Am.* **83**, 352–
553 370 (1990).

554 27. D. C. S. G. Oliveira *et al*., Identification and characterization of the *doublesex* gene of
555 *Nasonia*. *Insect Mol. Biol.* **18**, 315–324 (2009).

556 28. E. C. Verhulst, L. W. Beukeboom and L. van de Zande, Maternal control of haplodiploid
557 sex determination in the wasp *Nasonia*. *Science.* **328**, 620–623 (2010).

558 29. B. S. Baker and M. F. Wolfner, A molecular analysis of *doublesex*, a bifunctional gene that
559 controls both male and female sexual differentiation in *Drosophila melanogaster*. *Genes Dev.*
560 **2**, 477–489 (1988).

561 30. J. N. Shukla and J. Nagaraju, Two female-specific DSX proteins are encoded by the sex-
562 specific transcripts of *dsx*, and are required for female sexual differentiation in two wild
563 silkmoth species, *Antheraea assama* and *Antheraea mylitta* (Lepidoptera, Saturniidae). *Insect*
564 *Biochem. Mol. Biol.* **40**, 672–682 (2010).

565 31. F. Nunes *et al*., Non-target effects of green fluorescent protein (GFP)-derived double-
566 stranded RNA (dsRNA-GFP) used in honey bee RNA interference (RNAi) assays, *Insects* **4**,
567 90–103 (2013).

568 32. E. H. Slifer, Sense organs on the antenna of a parasitic wasp, *Nasonia vitripennis*
569 (Hymenoptera, Pteromalidae). *Biol. Bull.* **136**, 253–263 (1969).

570 33. J. H. Massey and P. J. Wittkopp, The genetic basis of pigmentation differences within and
571 between *Drosophila* species. *Curr. Top. Dev. Biol.* **119**, 27-61.

572 34. D. W. Loehlin *et al*., Non-coding changes cause sex-specific wing size differences
573 between closely related species of *Nasonia*, *PLoS Genet.* **6**, e1000821 (2010).

574 35. D. W. Loehlin and J. H. Werren, Evolution of shape by multiple regulatory changes to a
575 growth gene. *Science* **335**, 943–7 (2012).

576 36. K. Mysore *et al*., siRNA-mediated silencing of *doublesex* during female development of
577 the dengue vector mosquito *Aedes aegypti*. *PLoS Negl. Trop. Dis.* **9**, e0004213 (2015).

578 37. R. E. Snodgrass, A revised interpretation of the external reproductive organs of male
579 insects. *Smithson. Misc. Collect.* **136**, 1–60 (1957).

580 38. A. E. Christiansen, E. L. Keisman, S. M. Ahmad and B. S. Baker, Sex comes in from the
581 cold: the integration of sex and pattern. *Trends Genet.* **18**, 510–516 (2002).

582 39. J.-C. Zhuo *et al*., Identification and functional analysis of the *doublesex* gene in the sexual
583 development of a hemimetabolous insect, the brown planthopper. *Insect Biochem. Mol. Biol.*
584 **102**, 31–42 (2018).

585 40. S. Baral, G. Arumugam, R. Deshmukh and K. Kunte, Genetic architecture and sex-
586 specific selection govern modular, male-biased evolution of *doublesex*. *Sci. Adv.* **5**, eaau3753
587 (2019).

588 41. Y. Yang, W. Zhang, J. R. Bayrer and M. A. Weiss, Doublesex and the regulation of sexual
589 dimorphism in *Drosophila melanogaster*. *J. Biol. Chem.* **283**, 7280–7292 (2008).

590 42. K. Tamura, J. Dudley, M. Nei and S. Kumar, MEGA4: Molecular evolutionary genetics
591 analysis (MEGA) software version 4.0. *Mol. Biol. Evol.* **24**, 1596–1599 (2007).

592 43. J. H. Werren, D. W. Loehlin and J. D. Giebel, Larval RNAi in *Nasonia* (parasitoid wasp).
593 *Cold Spring Harb. Protoc.* DOI:10.1101/pdb.prot5311 (2009).

594 44. J. A. Lynch and C. Desplan, A method for parental RNA interference in the wasp *Nasonia*
595 *vitripennis*. *Nat. Protoc.* **1**, 486–494 (2006).

596 45. W. D. Hamilton, Extraordinary sex ratios. *Science.* **156**, 477–488 (1967).

597 46. D. W. Loehlin, L. S. Enders and J. H. Werren, Evolution of sex-specific wing shape at the
598 widerwing locus in four species of *Nasonia*. *Heredity.* **104**, 260–269 (2010).

599 47. H. C. J. Godfray, Parasitoids: behavioral and evolutionary ecology. *Parasitoids Behav.*
600 *Evol. Ecol.* (1994).

601 48. N.-Y. Liu *et al*., Morphology and ultrastructure of the male reproductive system of the
602 jewel wasp, *Nasonia vitripennis* (Walker) (Hymenoptera: Pteromalidae). *J. Asia. Pac. Entomol.*
603 **20**, 577–582 (2017).

604 49. C. Ramakers, J. M. Ruijter, R. H. L. Deprez and A. F. Moorman, Assumption-free analysis
605 of quantitative real-time polymerase chain reaction (PCR) data. *Neurosci. Lett.* **339**, 62–66
606 (2003).

607 **Figures**

608

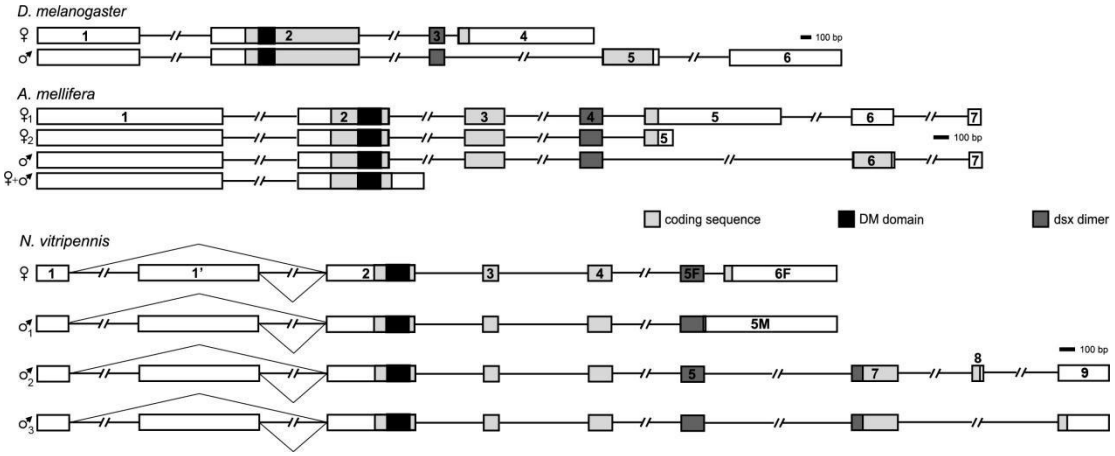

609

610 Figure 1. Comparison of insect *Doublesex* (*Dsx*) gene models. The eight *N. vitripennis* male
611 and female *Dsx* splice variants are compared to *Dsx* splice variants of *D. melanogaster* and *A.*
612 *mellifera*. Figure was modified from Oliveira *et al.* (27) to include the alternative 1st exon (1')
613 and the additional *NvDsx* male splice variants. Male and female specific splice forms are
614 indicated by ♂ and ♀. Exon numbers are noted on each exon. Light grey, black and dark grey
615 blocks indicate coding region, DM domain and OD2 Dsx dimer region respectively. Scales are
616 provided behind each species splice structures.

617

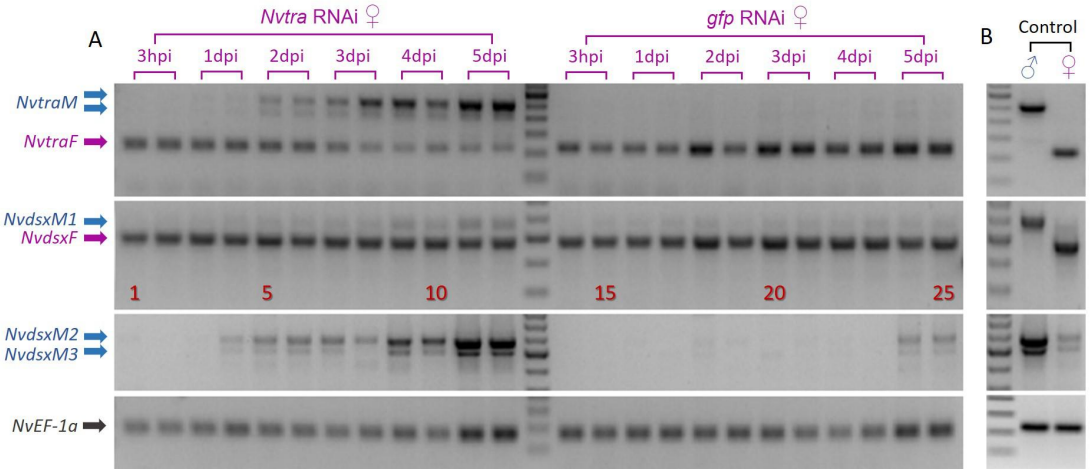

618

619 Figure 2. Confirmation of sex-specific *Dsx* splicing after *Nvtra* knockdown in *N.vitripennis.* (A)
620 Sex-specific splice variants of *Nvtra* and *NvDsx* in *N. vitripennis* females that are injected in
621 the 4th instar larval stage with *Nvtra* dsRNA or *gfp* dsRNA. (B) Male and female non-treated
622 (NT) control samples for each primer sets. Arrows indicate male (in blue) and female (in
623 purple) splice forms of the different genes. Lanes 1-12: Female *Nvtra* knockdown samples
624 from 3-hour post injection (hpi) to 5-day post injection (dpi). Lane 13: 100bp ladder (Thermo).
625 Lanes 14-25: Female *gfp* knockdown samples from 3dpi to 5dpi. For each stage two samples
626 are used. *NvEF-1a* is used as expression and loading control.

627

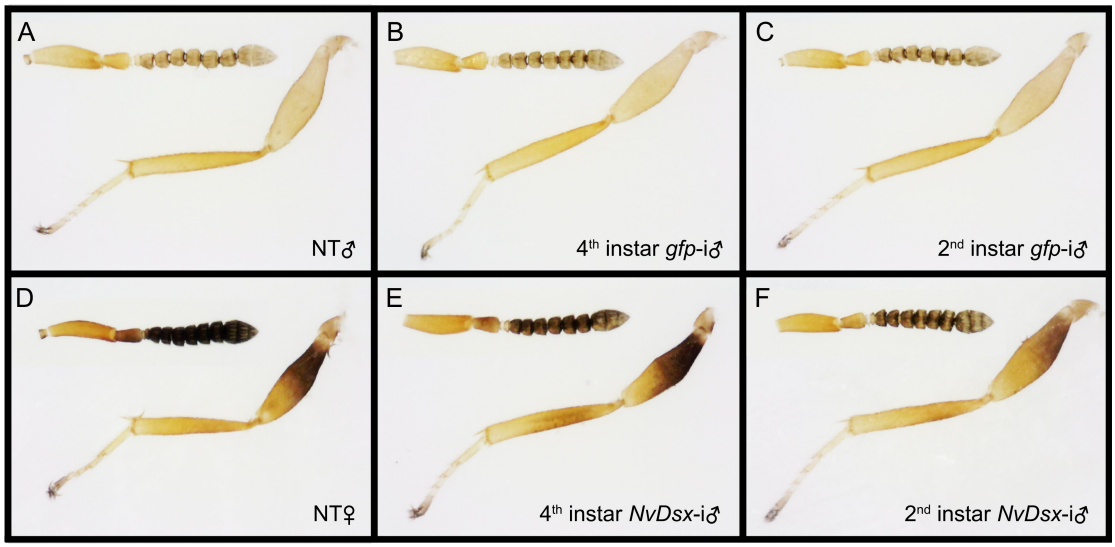

Figure 3. Pigmentation of antennae and hind legs of adult wasps after *NvDsx* or *gfp* dsRNA treatment in different developmental stages. (A) non-treated (NT) male (B) 4th instar *gfp* RNAi (*gfp*-i) male (C) 2nd instar *gfp*-i male (D) NT female (E) 4th instar *NvDsx* RNAi (*NvDsx*-i) male and (F) 2nd instar *NvDsx*-i male. Light source and exposure time are equal for all pictures.

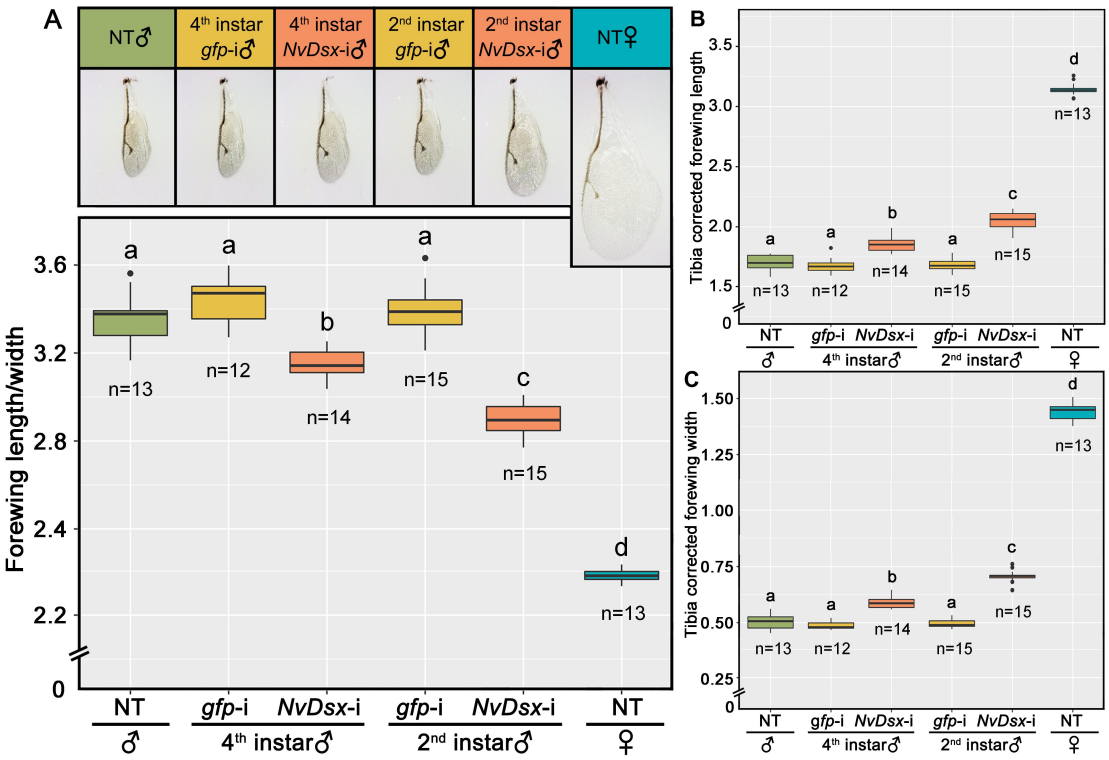

634

635 Figure 4. Comparison of forewing size of adult after *NvDsx* or *gfp* dsRNA treatment in the 2nd
636 or 4th larval instar males and non-treated control. Y-axis represents: (A) Forewing length/width
637 ratio corrected with tibia length, (B) Length corrected with tibia length, (C) Width corrected
638 with tibia length. X-axis shows six different groups: males treated with dsRNA of *NvDsx*
639 (*NvDsx*-i) and *gfp* (*gfp*-i) in the 2nd and 4th larval instar, non-treated (NT) males and NT
640 females. Boxplots were generated in R and display minimum, first quartile (Q1), median, third
641 quartile (Q3), and maximum. Dots outside the boxplots represent outliers. Replicates are
642 provided in the figures of each treatment. One-way ANOVA and post-hoc Tukey's HSD were
643 used for data analysis. Letters in the figures denote statistical significance ($P<0.05$) among
644 treatments.

645

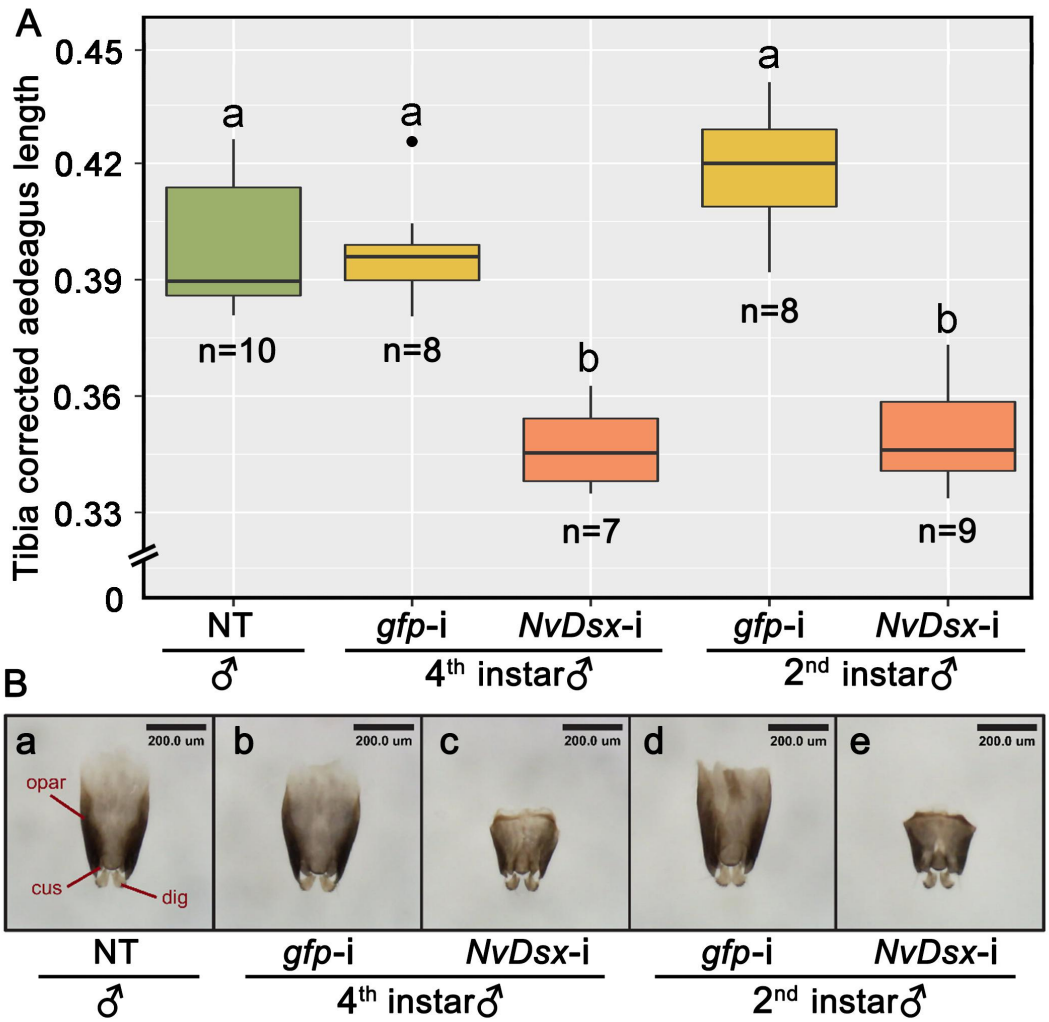

Figure 5. Comparison of external reproduction organs in males of different treatments. (A) Comparison of genitalia length of adult males treated with dsRNA of *NvDsx* (*NvDsx*-i) or *gfp* (*gfp*-i) in the 2nd or 4th larval instar males and non-treated (NT) control males. Y-axis represents genitalia length corrected with tibia length. Boxplots were generated in R and display minimum, first quartile (Q1), median, third quartile (Q3), and maximum. Dots outside the boxplot represent outliers. One-way ANOVA and post hoc Tukey's HSD were used for data analysis. Letters in the figures denote statistical significance ($P<0.05$) among treatments. (B) Comparison of paramere length (without aedeagus) of adult males after *NvDsx* or *gfp* dsRNA treatment in the 2nd or 4th larval instar and NT control. (a) paramere structure (without aedeagus) in NT males, (b and d) 4th and 2nd larval instar *gfp*-i males, (c and e) 4th and 2nd larval instar *NvDsx*-i males. Each paramere component is described in *E. Snodgrass (1957)* (37) and labeled with the following abbreviations: outer paramere (opar), cuspis (cus) and digitus (dig).

669

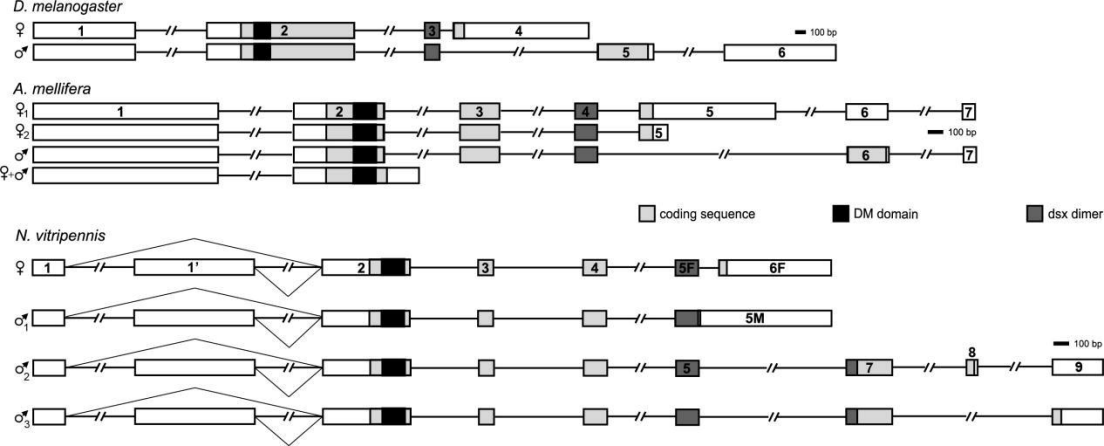
D. melanogaster
♀
♂
1
2
3
4
5
6
100 bp
A. mellifera
♀1
♀2
♂
♀1/♂
1
2
3
4
5
6
7
100 bp
coding sequence
DM domain
dsx dimer
N. vitripennis
♀
♂1
♂2
♂3
1
1'
2
3
4
5F
6F
5M
5
7
8
9
100 bp

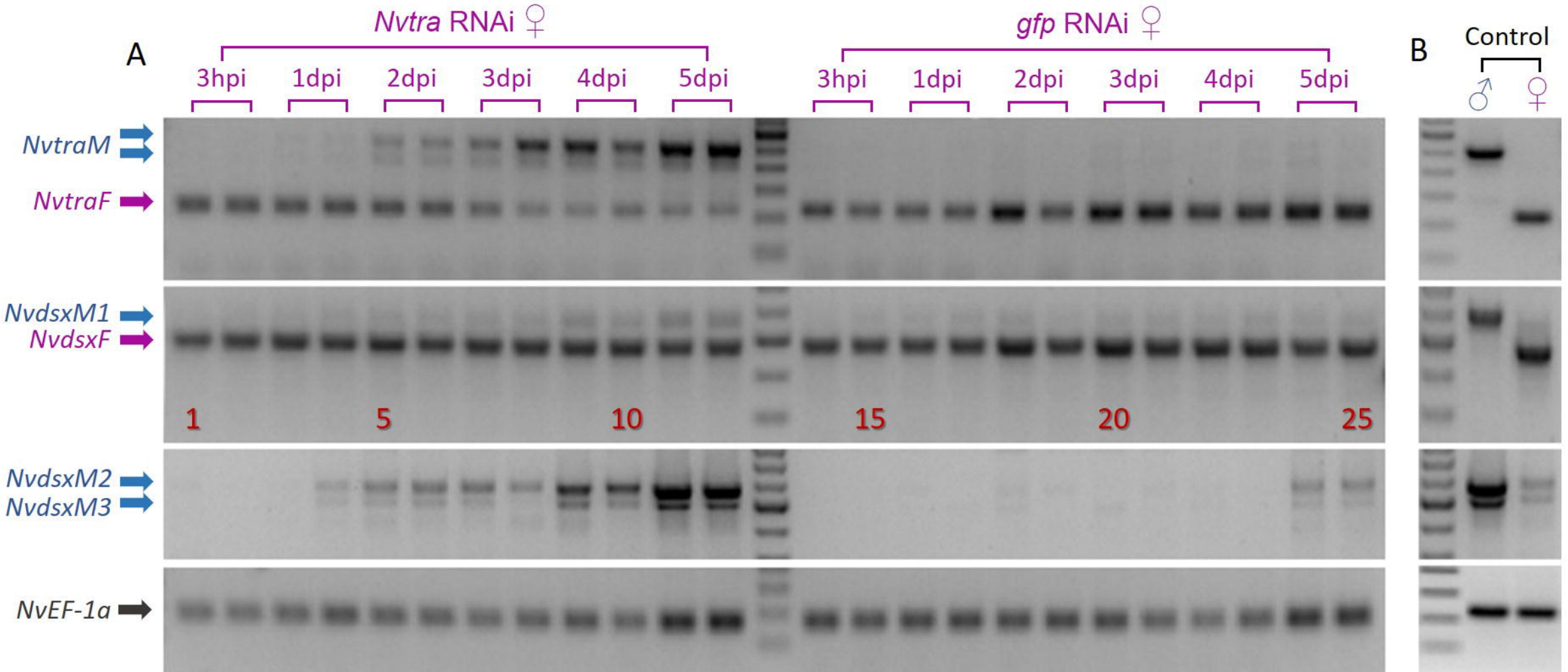
A
Nvtra RNAi ♀
gfp RNAi ♀
3hpi
1dpi
2dpi
3dpi
4dpi
5dpi
B
Control
♂
♀
NvtraM
NvtraF
NvdsxM1
NvdsxF
NvdsxM2
NvdsxM3
NvEF-1a
1
5
10
15
20
25

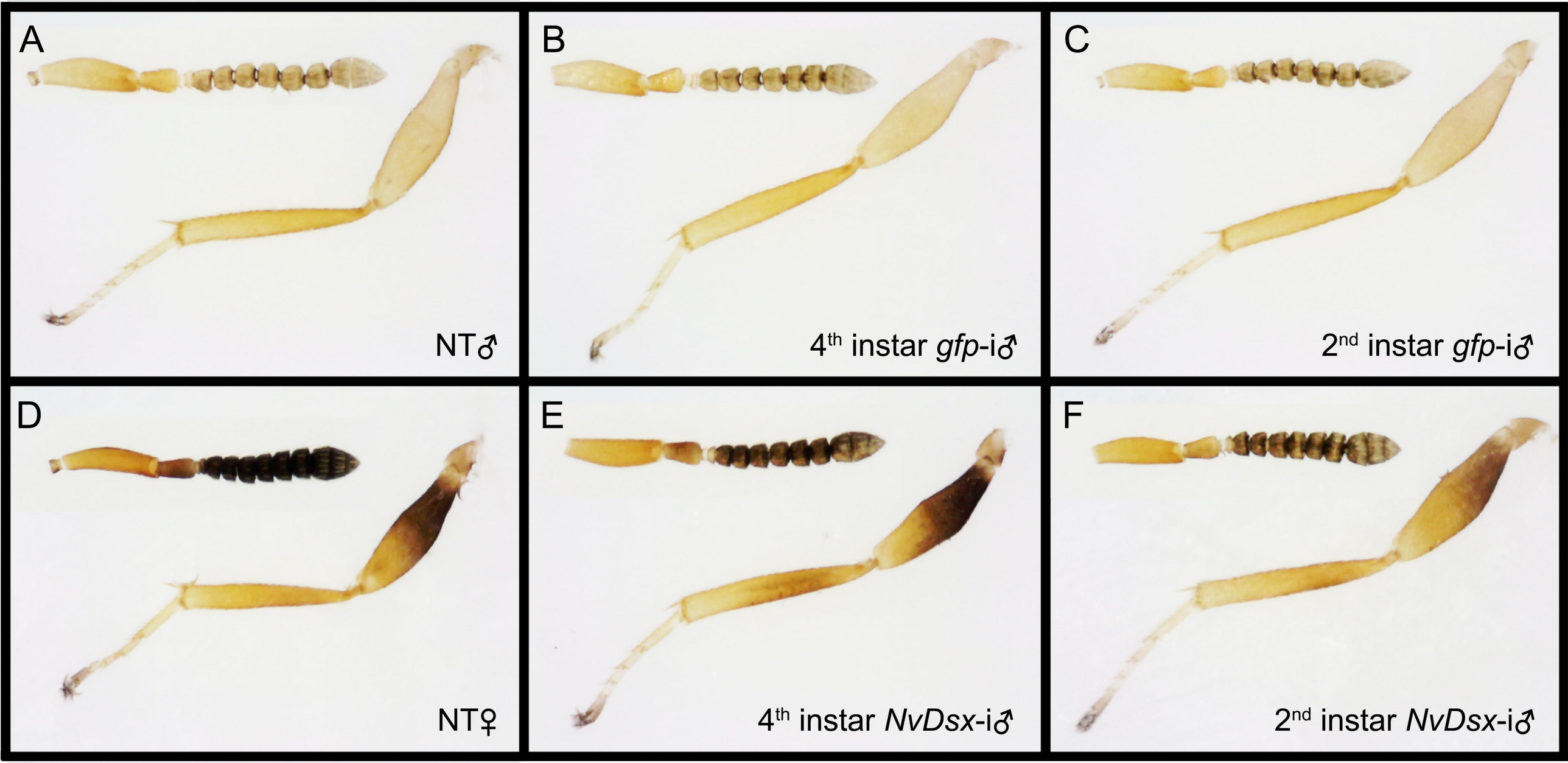
A
NT♂
B
4th instar gfp-i♂
C
2nd instar gfp-i♂
D
NT♀
E
4th instar NvDsx-i♂
F
2nd instar NvDsx-i♂

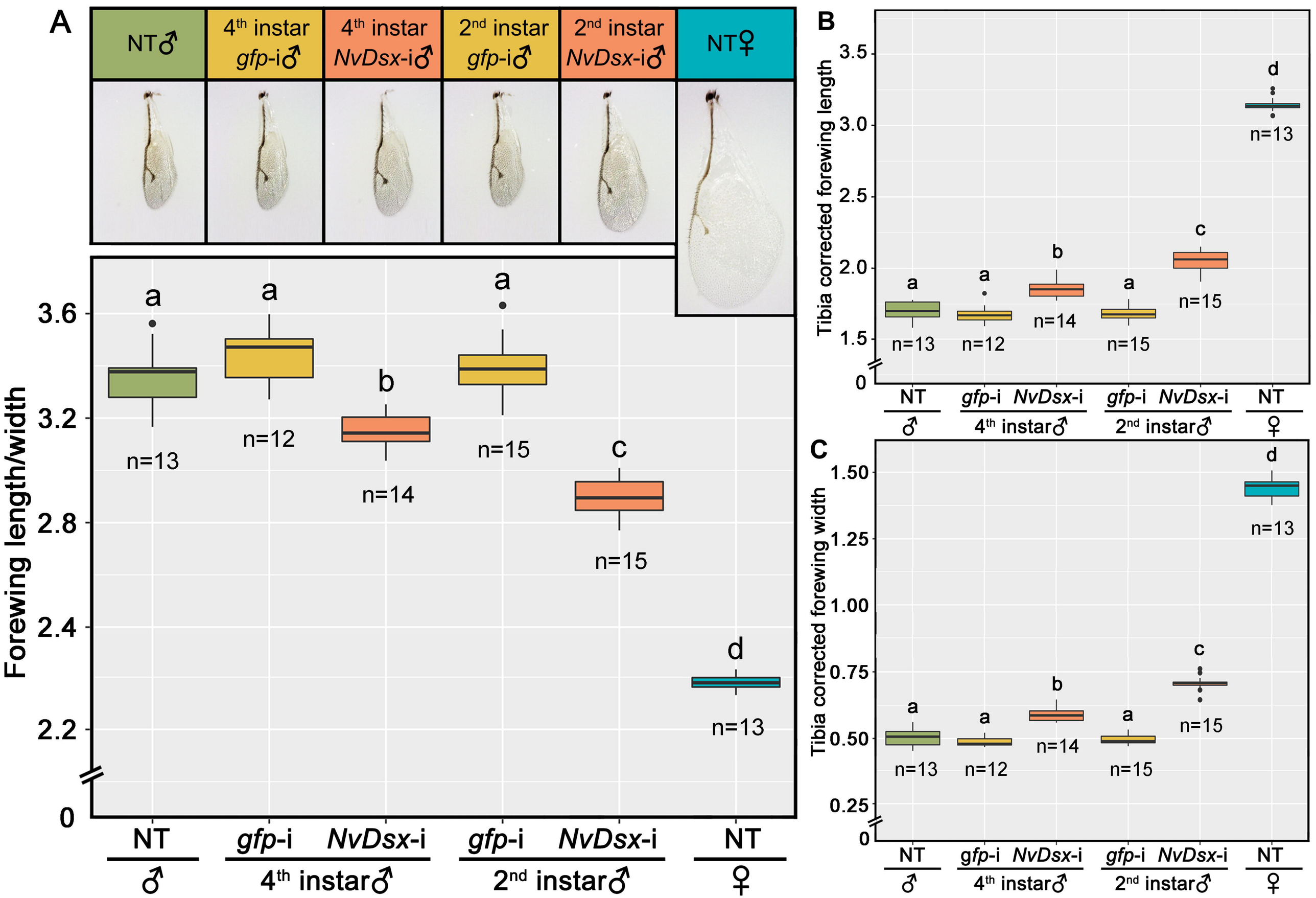
A
NT♂
4th instar gfp-i♂
4th instar NvDsx-i♂
2nd instar gfp-i♂
2nd instar NvDsx-i♂
NT♀
Forewing length/width
3.6
3.2
2.8
2.4
2.2
0
a
a
b
a
c
d
n=13
n=12
n=14
n=15
n=15
n=13
NT
gfp-i
NvDsx-i
gfp-i
NvDsx-i
NT
♂
4th instar♂
2nd instar♂
♀
B
Tibia corrected forewing length
3.5
3.0
2.5
2.0
1.5
0
a
a
b
a
c
d
n=13
n=12
n=14
n=15
n=15
n=13
NT
gfp-i
NvDsx-i
gfp-i
NvDsx-i
NT
♂
4th instar♂
2nd instar♂
♀
C
Tibia corrected forewing width
1.50
1.25
1.00
0.75
0.50
0.25
0
a
a
b
a
c
d
n=13
n=12
n=14
n=15
n=15
n=13
NT
gfp-i
NvDsx-i
gfp-i
NvDsx-i
NT
♂
4th instar♂
2nd instar♂
♀

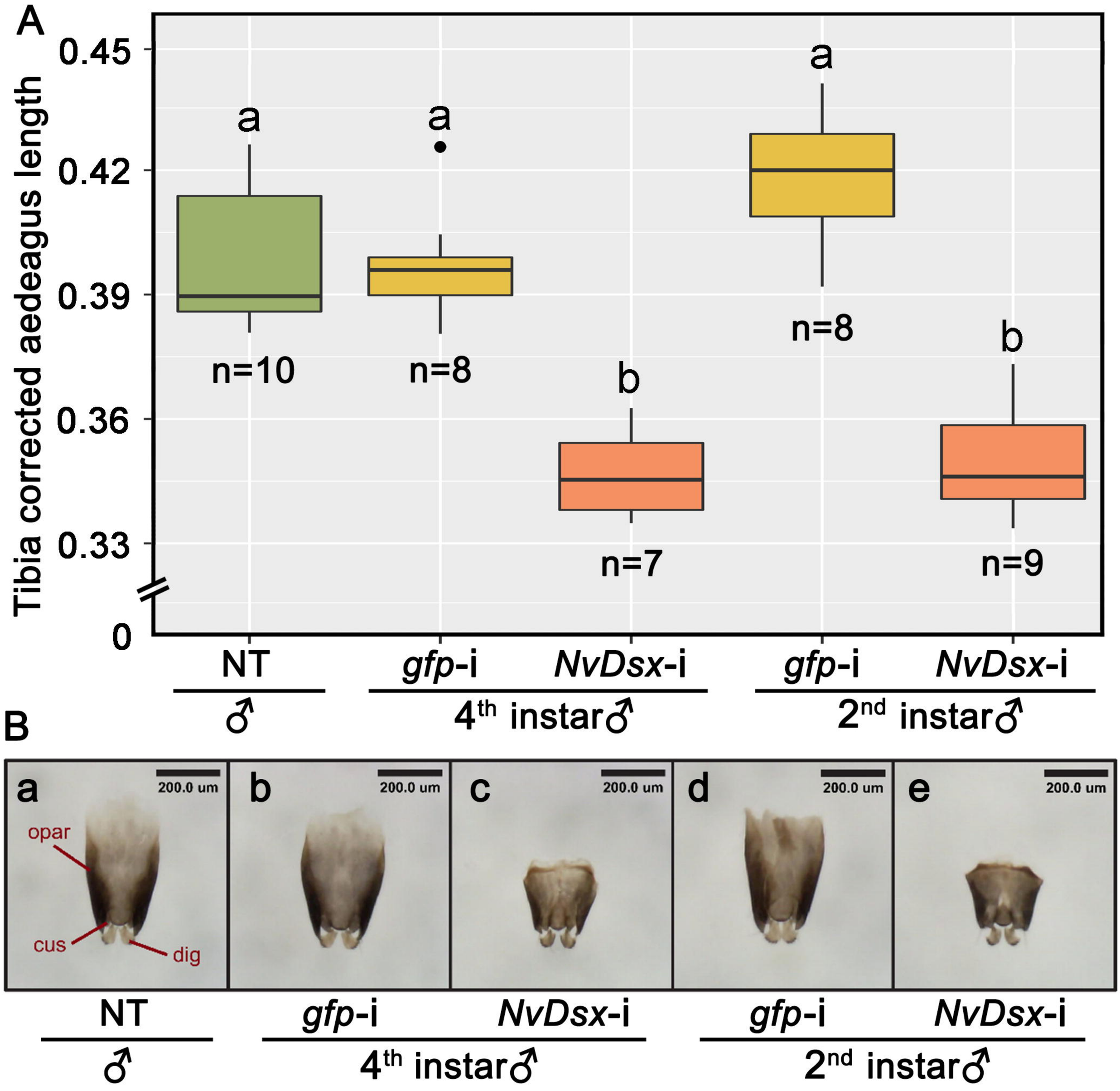
A
Tibia corrected aedeagus length
0.45
0.42
0.39
0.36
0.33
0
a
a
a
b
b
n=10
n=8
n=8
n=7
n=9
NT
gfp-i
NvDsx-i
gfp-i
NvDsx-i
♂
4th instar♂
2nd instar♂
B
a
b
c
d
e
200.0 um
opar
cus
dig
NT
gfp-i
NvDsx-i
gfp-i
NvDsx-i
♂
4th instar♂
2nd instar♂

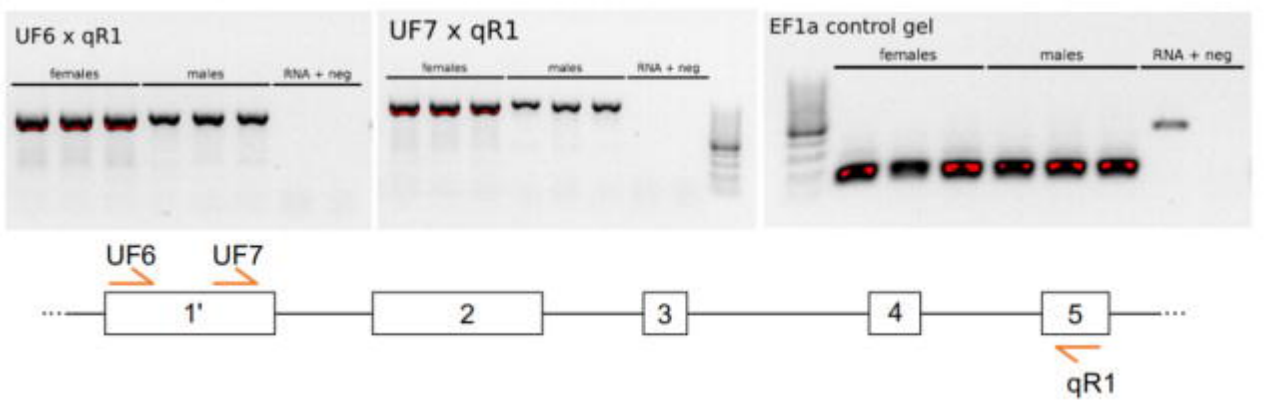
UF6 x qR1
females
males
RNA + neg
UF7 x qR1
females
males
RNA + neg
EF1a control gel
females
males
RNA + neg
UF6
UF7
1'
2
3
4
5
qR1

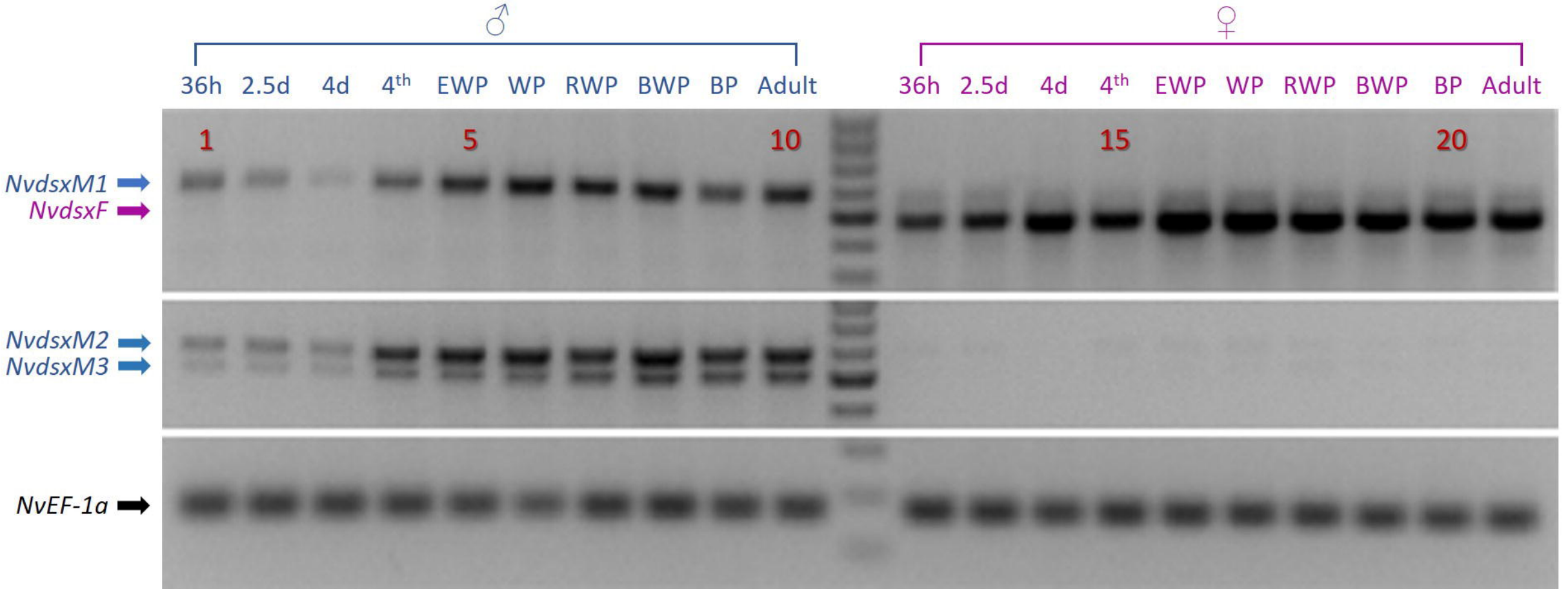
♂
♀
36h
2.5d
4d
4th
EWP
WP
RWP
BWP
BP
Adult
1
5
10
15
20
NvdsxM1
NvdsxF
NvdsxM2
NvdsxM3
NvEF-1a

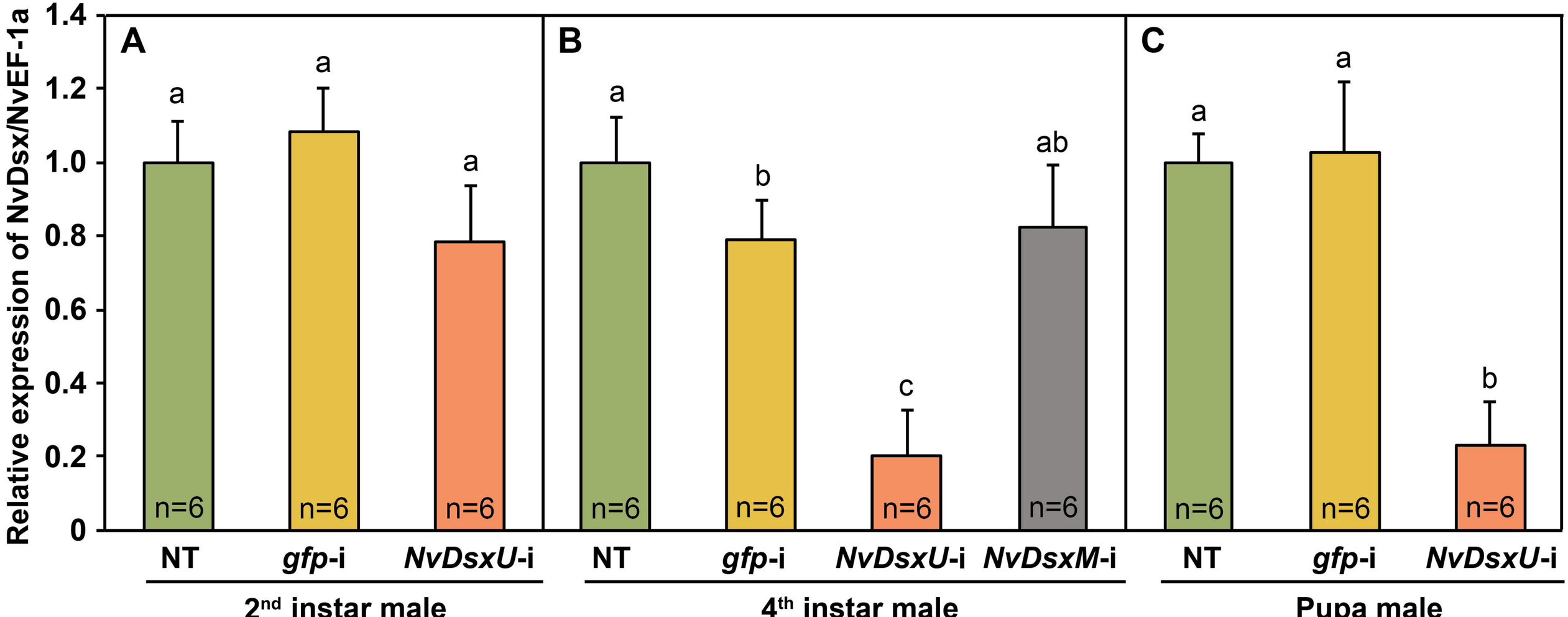
Relative expression of NvDsx/NvEF-1a
1.4
1.2
1.0
0.8
0.6
0.4
0.2
0
A
B
C
a
a
a
a
b
c
ab
a
a
b
n=6
NT
gfp-i
NvDsxU-i
NvDsxM-i
2nd instar male
4th instar male
Pupa male

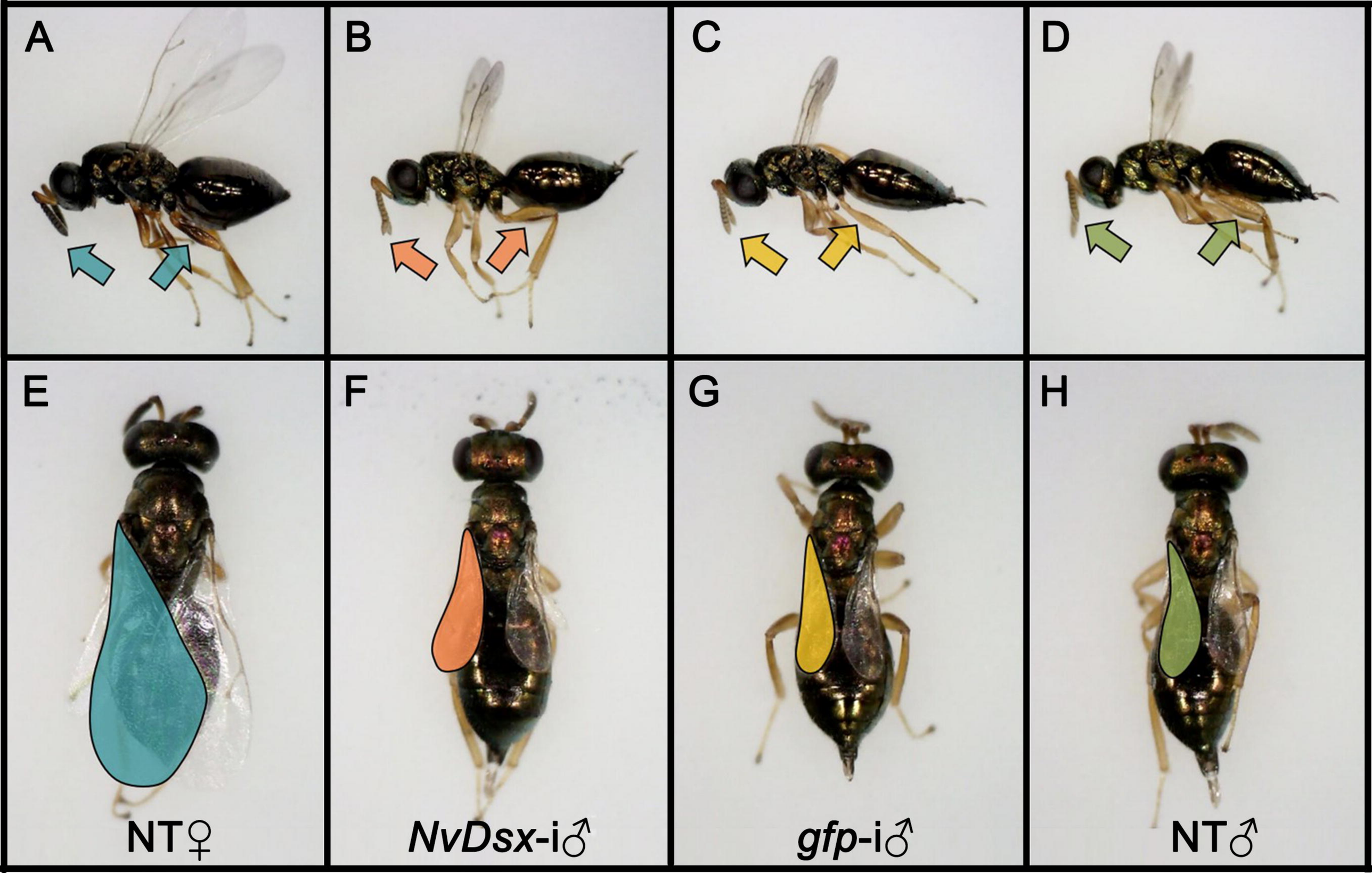
A
B
C
D
E
F
G
H
NT♀
NvDsx-i♂
gfp-i♂
NT♂

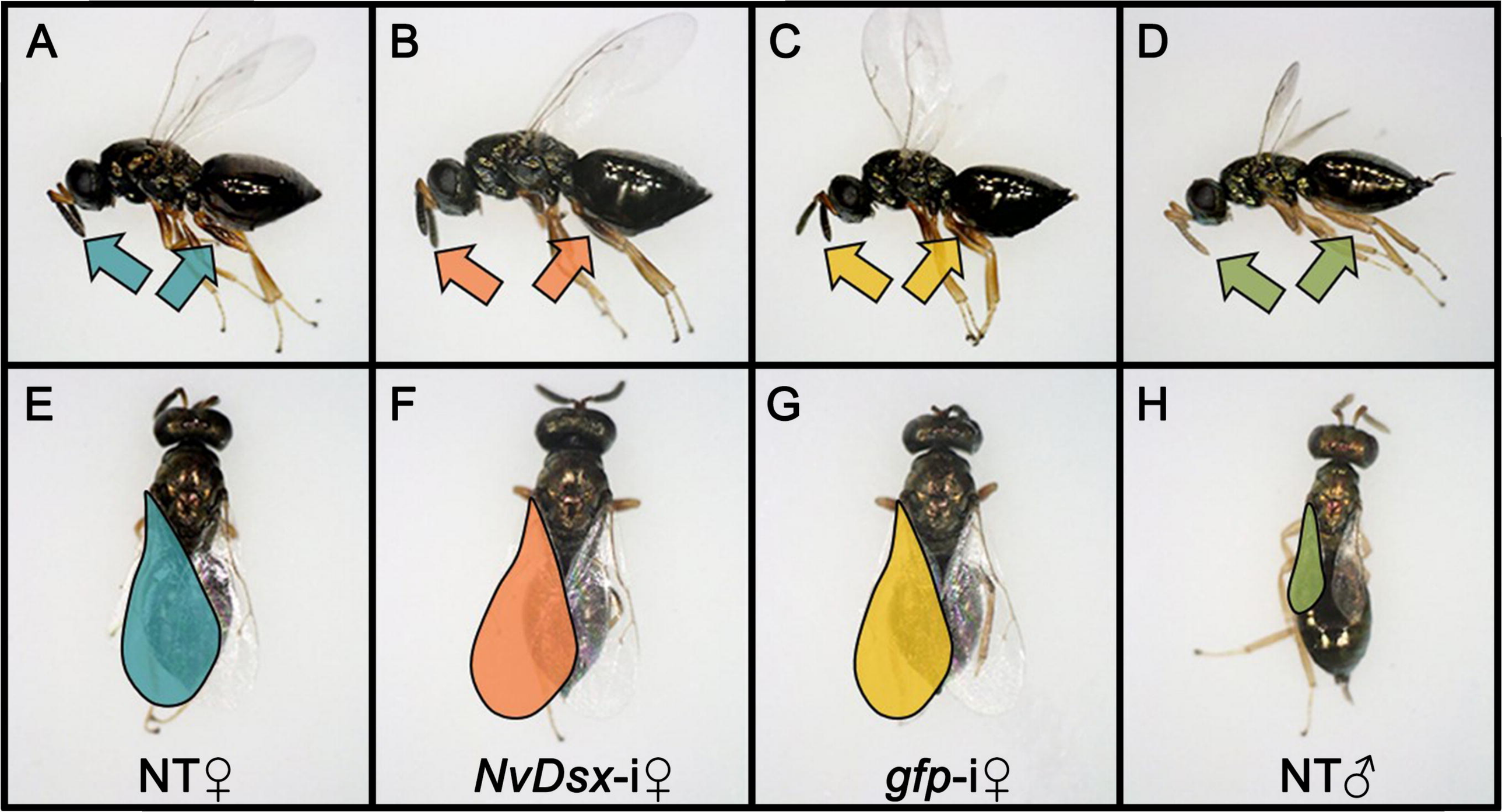
A
B
C
D
E
F
G
H
NT♀
NvDsx-i♀
gfp-i♀
NT♂

A

common OD2 domain | male OD2

1. Apis_mellifera_M(NP_001104725)
2. Asobara_tabida_M(ATE86740)
3. Athalia_rosae_M(*)
4. Nasonia_vitripennis_M2(XP_008205424)
5. Nasonia_vitripennis_M3(XP_008205423)
6. Nasonia_vitripennis_M1(NP_001155989)
7. Trichomalopsis_dubius_M(ACJ65506)
8. Drosophila_melanogaster_M(NP_731197)
9. Musca_domestica_M(AAR23813)
10. Lucilia_cuprina_M(ADG37648)
11. Ceratitis_capitata_M(AAN63597)
12. Bactrocera_dorsalis_M(ACN73399)
13. Anastrepha_obliqua_M(AAY25167)
14. Anopheles_gambiae_M(AAZ78362)
15. Aedes_aegypti_M(ABD96573)
16. Culex_quinquefasciatus_M(AJB28477)
17. Antheraea_mylitta_M(ADL40855)
18. Bombyx_mori_M(NP_001104815)
19. Helicoverpa_armigera_M(AHF81649)
20. Ostrinia_furnacalis_M(AHF81635)
21. Tribolium_castaneum_M(AFQ62105)
22. Cyclommatus_metallifer_finae_A(BAO23808)
23. Cyclommatus_metallifer_finae_B(BAO23809)
24. Onthophagus_taurus_M(AEX92938)
25. Nilaparvata_lugens_M(AWJ25055)

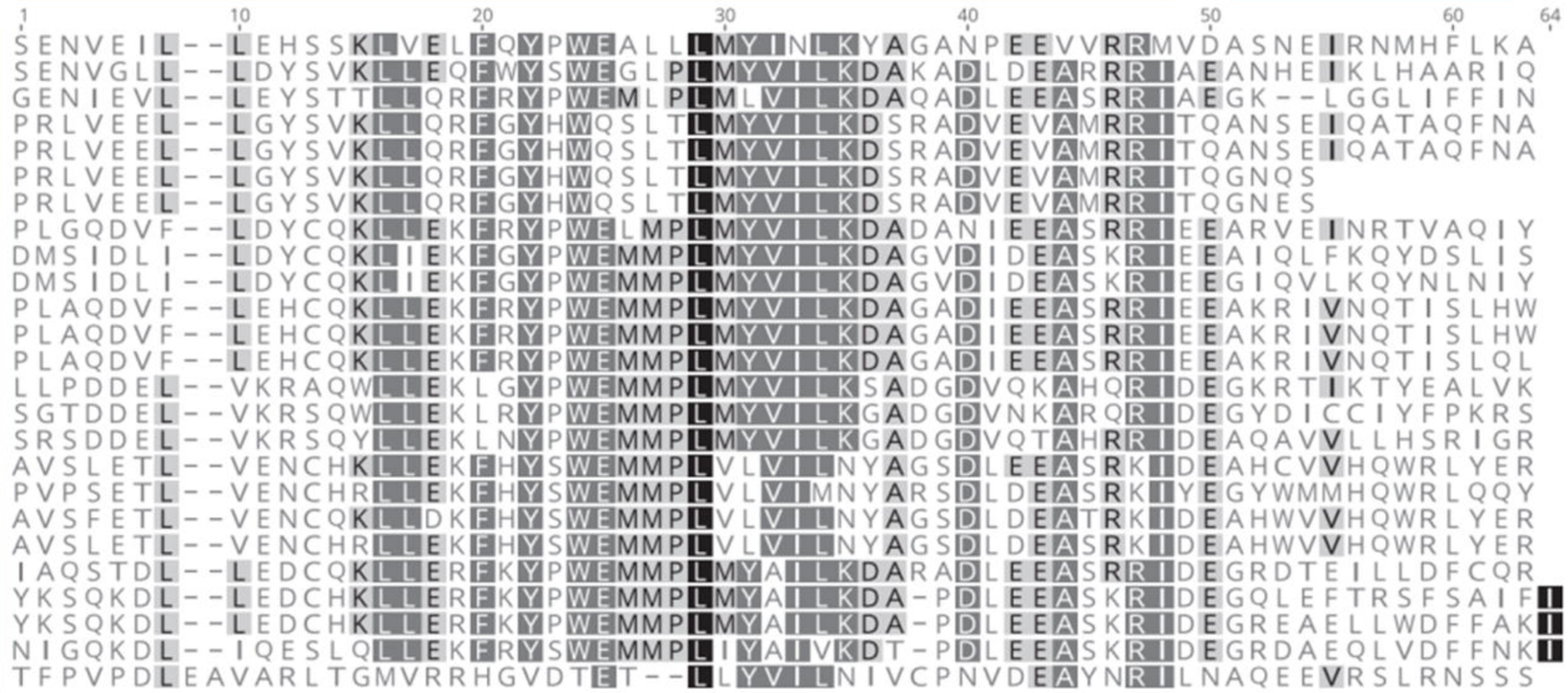

B

common OD2 domain | female OD2
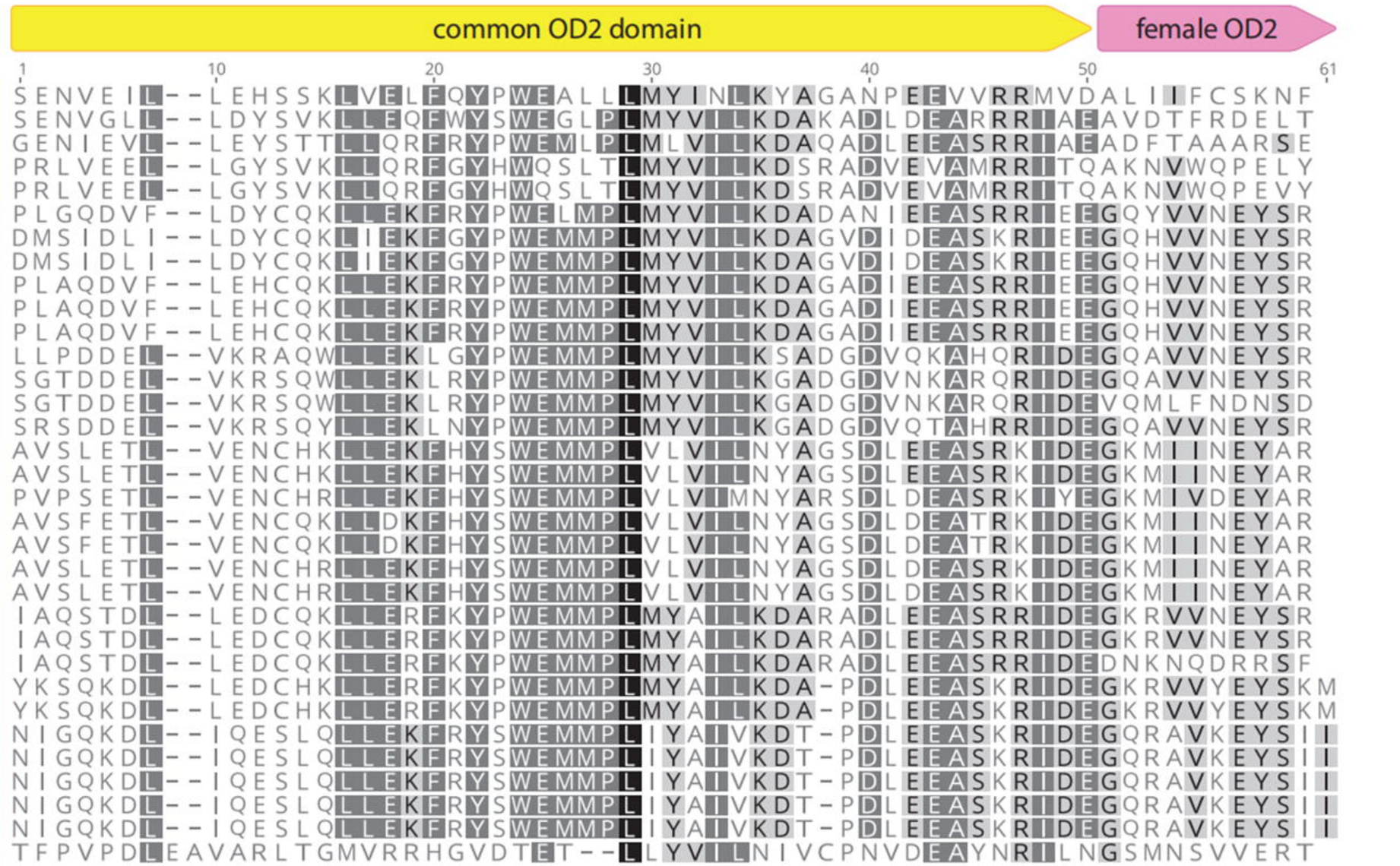
1. Apis_mellifera_F(NP_001128407)
2. Asobara_tabida_F(ATE86739)
3. Athalia_rosae_X1(XP_012262256)
4. Nasonia_vitripennis_F(NP_001155990)
5. Trichomalopsis_dubius_F(ACJ65505)
6. Drosophila_melanogaster_F(NP_731198)
7. Musca_domestica_F(AAR23812)
8. Lucilia_cuprina_F(ADG37649)
9. Ceratitis_capitata_F(AAN63598)
10. Bactrocera_dorsalis_F(AAV85891)
11. Anastrepha_obliqua_F(AAY25166)
12. Anopheles_gambiae_F(AAZ78363)
13. Aedes_aegypti_F1(ABD96571)
14. Aedes_aegypti_F2(ABD96572)
15. Culex_quinquefasciatus_F(AJB28478)
16. Antheraea_mylitta_F1(ADL40853)
17. Antheraea_mylitta_F2(ADL40854)
18. Bombyx_mori_F(NP_001036871)
19. Helicoverpa_armigera_F1(AHF81652)
20. Helicoverpa_armigera_F2_(AHF81653)
21. Ostrinia_furnacalis_F1(AHF81640)
22. Ostrinia_furnacalis_F2(AHF81641)
23. Tribolium_castaneum_F1(AFQ62106)
24. Tribolium_castaneum_F2(AFQ62107)
25. Tribolium_castaneum_F3(AFQ62108)
26. Cyclommatus_metallifer_finae_C(BAO23810)
27. Cyclommatus_metallifer_finae_D(BAO23811)
28. Onthophagus_taurus_F1(AEX92939)
29. Onthophagus_taurus_F2(AEX92940)
30. Onthophagus_taurus_F3(AEX92941)
31. Onthophagus_taurus_F4(AEX92942)
32. Onthophagus_taurus_F5(AEX92943)
33. Nilaparvata_lugens_F(AWJ25056)